AD-A167 661 FEASIBILITY STUDY OF SURVEILLANCE AVOIDANCE DURING THE 1/1
DEPLOYMENT OF SOVI..(U) AIR FORCE INST OF TECH
WRIGHT-PATTERSON AFB OH SCHOOL OF ENGI.. E F FAUDREE
UNCLASSIFIED DEC 85 AFIT/GSO/ENS/85D-9 F/G 17/9 NL

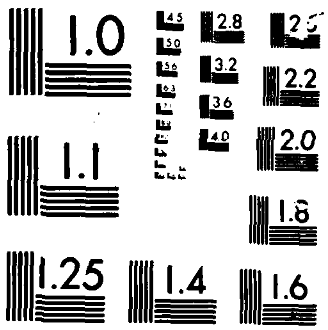

MICROCOP CHART

AFIT/GSO/ENS/85D-9

FEASIBILITY STUDY OF SURVEILLANCE
AVOIDANCE DURING THE DEPLOYMENT OF
SOVIET PAYLOADS OF MILITARY INTEREST
INTO ORBIT FROM A SOVIET SHUTTLE

THESIS

Edward F. Faudree, Jr.
Captain, USAF
AFIT/GSO/ENS/85D-9

Approved for public release; distribution unlimited

AFIT/GSO/ENS/85D-9

FEASIBILITY STUDY OF SURVEILLANCE AVOIDANCE DURING THE DEPLOYMENT OF SOVIET PAYLOADS OF MILITARY INTEREST INTO ORBIT FROM A SOVIET SHUTTLE

THESIS

Presented to the Faculty of the School of Engineering

of the Air Force Institute of Technology

Air University

In Partial Fulfillment of the

Requirements for the Degree of

Master of Science in Space Operations

Edward F. Faudree, Jr., B.A.

Captain, USAF

December, 1985

<u>Preface</u>

The purpose of this study was to start a line of inquiry into how well the North American Aerospace Defense Command's (NORAD) radars can detect the deployment of satellites from a Soviet space shuttle. Little work has been done at HQ NORAD on this problem. It may be several years before the U.S.S.R. attempts to use a shuttle vehicle to place satellites into orbit, but the U.S. should be prepared for this activity.

My first tour of duty in the Air Force was at the NORAD Cheyenne Mountain Complex, where I worked as an orbital analyst. Part of that job was the detection and cataloging of new satellites placed in orbit. Soviet launches that did not fit any historical profile were a source of worry; we wanted to be sure we could always detect any change in the satellite's orbit.

I thank Maj William F. Rowell, my faculty advisor, for his reading and re-reading of this thesis, suggesting changes and additions to make the analysis I did clear in the mind of the reader. I also thank Lt Col J. Widhalm, who served as my reader, for his effort in keeping the work technically correct. I appreciate the assistance from Maj James Bray, HQ NORAD/DOSS, for providing ideas and documents used in this thesis.

Finally, I gratefully thank my wife Vicki for her patience and caring during the months I worked on this thesis.

Edward F. Faudree, Jr.

Page 23 does not contain classified information.
Per Ms. Melonie Dahmer, AFIT/EN

Table of Contents

List of Figures

Figure | Page

List of Tables

Table | Page

Abstract

This work concerns how easily the North American Aerospace Defense Command's (NORAD) radars can detect a satellite deployment from a Soviet space shuttle, one that is comparable to the U.S. space shuttle in size and capability. The radar locations and capabilities were assumed to be the ones presently operating plus a new PAVE PAWS radar in Texas and a new mechanical tracker on the island of Saipan. All radars were assumed to be in working order, and tracking the shuttle.

The shuttle was assumed to be launched in a 51.62° inclination, and would attempt deployment only at an ascending or descending node. The satellite could move away from the shuttle along the shuttle's radius vector, velocity vector, or angular momentum vector, so that it is approximately 50 kilometers from the shuttle one half an orbital revolution later. The geocentric angular separation, absolute distance apart and range difference is calculated when the pair are closest to the radar. The elevation angle above the radar's horizon is estimated, and assuming the worst-case viewing geometry of the shuttle and satellite by the radar site, a topocentric range difference and angular separation are determined. These values of angle and distance are compared to that particular radar's capabilities and if the range and angle are much larger, approximately equal to, or less, than the sensor's limiting range and beamwidth, then the probability of detection is labeled high, medium or low, respectively. This determines the best opportunities the USSR has to deploy a satellite undetected by U.S. radars. The first 30 orbital revolutions are so examined. An orbital maneuver burn of a naval surveillance satellite at a selected deployment opportunity is tested, leading to its detection by the next radar that has an opportunity to view the shuttle and satellite.

This leads to the conclusion that the USSR has little chance to deploy a satellite by a space shuttle and have it go undetected, if the NORAD sensors are available for actively searching for this deployment.

Feasibility Study of Surveillance Avoidance during the Deployment of Soviet Payloads of Military Interest into Orbit from a Soviet Shuttle

Chapter One

Introduction

Background

The Union of Soviet Socialist Republics (U.S.S.R.) employs a different scheme from that of the United States in announcing spacecraft launches. Whereas the U.S. will for the most part announce many weeks in advance the launch of a spacecraft, the U.S.S.R. will announce a launch after it has occurred (certain Soyuz missions excepted). The announcement from the official Soviet news agency TASS may be issued several hours after the launch, and mission statements are often in very broad terms ("scientific advancement", "Earth resources", and the like). This secrecy makes the job at the North American Aerospace Defense Command (NORAD) Space Surveillance Center (NSSC) a very difficult one, because this center has the responsibility for observing, tracking and cataloging all man-made objects in Earth orbit.

The first indication of a launch from the U.S.S.R. is an alert message from one of our early warning satellites. The Missile Warning Center at the NORAD Cheyenne Mountain Complex must then quickly decide if this is an Intercontinental Ballistic Missile (ICBM) aimed at the U.S., a test of an ICBM, a sounding rocket, or a space launch. The rocket booster category must be determined, as well as the azimuthal heading. Once the Missile Warning Center identifies the launch as a space mission, with a booster type and heading, the NSSC is still faced with a number of possible missions to be performed by the unidentified spacecraft. The mission could be a peaceful, "civilian" one, or it could have a mission of military importance. The NSSC must also determine the mathematical description of the spacecraft's orbit, called the orbital element set. To do this last task, messages must be sent out to radar and optical tracking stations located throughout the world, requiring them to detect and track the new satellite. The observations are sent back to the NSSC in Cheyenne Mountain, and are reduced to the orbital element set. The element set aids in determining the mission, because historically, certain mission types go into certain types of orbits. If the spacecraft has a military mission, the NSSC must send additional messages to various Department of Defense units, in order to warn them that their location and mission may be observed by the satellite.

Although this is a lot of work to be accomplished in a very short period of time, it is done in a predetermined, step-by-step manner. An aid to this mammoth task is that launches for a particular mission follow an historical pattern; one launch is pretty much like another. This is true not only of the U.S.S.R., but to a lesser extent, of the United States as well. The U.S. does not normally announce impending launches of a military spacecraft, but since we do announce civilian ones, it is not difficult to determine that an unannounced launch is a military one, thereby making the task of the Soviet counterpart to the NSSC a bit easier in this regard. The Soviets would have a much smaller number of missions from which to choose, i.e., military missions only. Also, the U.S. has fewer types of boosters than the U.S.S.R., so there would be a smaller field of choices in classifing a booster type.

The historically predictable, clockwork pattern of a certain type of booster placing a certain type of payload into an initial "parking" orbit and then boosting into a final orbit at predetermined times may be phased out by the newest generation of spacecraft, the Space Shuttle. The U.S. Space Shuttle is capable of carrying several payloads into orbit at once, will be used to deploy many different mission payloads, including ones of military importance, and can inject payloads into the transfer orbit many hours after the inital launch of the shuttle. Earlier systems depended upon commands from ground stations, or simple mechanical timers, to boost satellites to the proper orbit; now the final decision rests with the autonomous crew aboard the shuttle as to when to launch a payload. Nor is this capability limited to the United States. According to Aviation Week and Space Technology, magazine, the Soviets are developing a version of the U.S. Space Shuttle, as well as a smaller "ferry" shuttle (8, 18-19; 9, 225-259; 10, 18-19; 21, 25). Although this smaller shuttle could deploy satellites in space, it appears the primary mission will be to ferry cosmonauts to and from Soviet space stations. The first manned launch of the smaller shuttle may be as early as this year (1985) (10, 18); the larger, heavy lift shuttle would probably not be launched until 1986 at the earliest (22, 21).

Fortunately, the laws of physics are the same for both unmanned expendable boosters and shuttles. If a nation desires to place a satellite into a particular orbit, there are still constraints on shuttle launch time and transfer orbit injection time. There is a greater flexibility with a shuttle vehicle, but the laws of celestial mechanics cannot be ignored. Instead, these laws can be used for planning and predicting the placement of certain satellite mission types into their unique orbits by a shuttle vehicle.

Specific issue

The U.S.S.R. has always desired to keep secret the launching time and mission identity of almost all of its space missions. By using a space shuttle, even the historical pattern of booster type and orbital inclination which gave clues to mission identity will be gone. The Soviets may use their shuttle to deploy a military-mission satellite into a new orbit, where it begins its operational life of reconnaissance / surveillance / intelligence gathering. The troubling aspect for the U.S. is that this satellite may be deployed without any indication to the North American Aerospace Defense Command's (NORAD) space surveillance tracking stations, which are located around the world. This may mean that the satellite can be in orbit for several hours without the U.S. knowing about it, and may damage national security by observing some U.S. military or experimental activities that would otherwise be concealed.

Specific problem statement

How feasible is it for the U.S.S.R. to deploy a satellite and inject it into an operational orbit without being observed by NORAD sensors?

Subsidiary research questions

1. What initial orbit will be used for the Soviet shuttle and what are the reasons for this choice?
2. Will the choice of this initial orbit have any effect on the type of satellite missions that can be deployed?
3. What are the times between sensor overflight by the Soviet shuttle for the different orbital revolutions?
4. How much of an opportunity for a hidden deployment do the range and angular resolution of the NORAD sensors afford?
5. What values for rating the probability of detecting the deployment

will be given and how will they be assigned?

6. What classes of Soviet military satellites will be examined?
7. What will be the method and orientation and velocity change maneuvers of the deployment?
8. How far away from the shuttle should the satellite be before the main maneuver burn occurs?

Scope of the Research

This thesis is a first attempt to determine if the U.S.S.R. could secretly deploy a satellite from a shuttle vehicle. As such, it provides an initial estimate for the possibility of a hidden Soviet satellite deployment, and offers a departure point for further analysis.

Shuttle and Satellite Orbits. The Soviet shuttle will be placed in an orbit that has been the nominal one for Soviet manned missions, and will stay in that orbit. It appears that the primary mission of the Soviet heavy shuttle is to support a manned presence in space, through space stations and a possible Mars mission (9, 257, 259). Therefore, the deployment of satellites would be a secondary mission. Only the deployed satellite will perform manuever firings, and only energy-conservative maneuvers will be used, such as the Hohmann transfer and orbital plane change manuever firings occurring at ascending and descending nodes. No orbital perturbations will be considered.

Ground Trace. The ground trace of the shuttle will be shown on a Mercator projection map provided by HQ SPACECOM / XPY. Only the initial shuttle orbit of 51.62° will be shown on the maps, to provide times of opportunity for the first step of satellite deployment.

NORAD Radar Sites. The only information about the various sensors used will be the sensor name, general location, radar type, range resolution and angular resolution. The sensor locations and surveillance areas are identified on the Mercator projection map.

Satellite Missions. There are many different missions of military interest, including photo-reconnaissance, radar calibration, communications, electronic signal gathering, and launch detection, but the mission examined here to illustrate the problem is naval reconnaissance. The satellites used for these missions have long orbital lifetimes for Soviet space systems, are not likely to maneuver during the operational lifespan, and can be easily boosted from the shuttle's orbit into the required orbit for the mission.

Literature Review

On 25 July 1985, a telephone conversation with Lt Col Eagan, HQ SPACECMD / DOSV, showed there is a strong interest and need to determine how readily a satellite deployment can be hidden from U.S. space surveillance sensors. Little actual work has been done on this, however, in either the Directorate of Operations or Future Plans (HQ SPACECMD / XPY) (11). Major James Bray of DOSS also expressed strong interest in the topic, and pointed out the lack of data collected and work accomplished by the intelligence / analysis community (6, 7).

While there has been no published works on using a Soviet shuttle as described in this work, there are a number of texts dealing with radar resolution (12; 14; 16; 18). These papers relate how to determine the normally computed angular resolution, and methods for improving the angular resolution of a radar, an important aspect for this study.

Thesis Overview

Chapter Two provides the explanation of the methodology used in the analysis. Operational assumptions are stated, and the information about the orbital path and sensor resolution is presented. Several Soviet satellites of interest are discussed, then the deployment process is described. The next major section concerns decision rules used to determine the probability of the radar detecting the deployed satellite.

Chapter Three presents the findings of the analysis. It provides the operating capabilities of the sensors, the Soviet shuttle orbital parameters, and the method of computing the satellite deployment velocities. Two tables show the times of opportunities the radars have to observe the shuttle and the probability of detecting the satellite.

Chapter Four summarizes the probabilities of detecting a deployment, identifies the best deployment opportunities, states the limitations of this analysis and makes a few recommendations for further study.

Chapter Two

Methodology

Explanation of Methodology

Operational Assumptions. A primary assumption used in this analysis is that the Soviet shuttle is very similar in capabilities to the U.S. shuttle. Design considerations seem to indicate this (9, 255-257). Another assumption is that all NORAD sensors will be operating and tracking the Soviet shuttle. There is the possibility that a non-operating sensor or a sensor that is busy tracking another object will provide greater opportunity for the Soviet shuttle to hide a satellite deployment. However, whether or not a sensor is "pre-occupied" or not operating would not be known sufficiently ahead of time to provide for mission planning, so this possibility will be ignored.

The Soviet shuttle will most probably be launched from the normal manned launch center of Tyuratam (a.k.a. Leninsk), on an azimuthal heading of 63.35 degrees, which places the shuttle in an orbital inclination of 51.62 degrees, the present Soviet manned spaceflight initial orbit inclination. The azimuth of 63.35° allows first stage boosters to fall into the northeast steppes of the U.S.S.R., rather than into neighboring countries. It is assumed that the shuttle will be in a circular orbit with an altitude of 310 kilometers (km), or 163 nautical miles. These are likely values and are easily achievable by the U.S. shuttle. These particular values were provided by Space Command (7). As mentioned in Chapter One, the Soviet shuttle's primary mission will be to support the Soviet space station or stations, or a possible Mars mission, and they are most likely to have this orbital inclination. The U.S.S.R. is building a shuttle partially for propaganda reasons ("The United States isn't the only one with a space shuttle."), but it does fit in well with the overall Soviet space strategy (6).

Orbital Path. Using the above orbital values, a map showing the detection limits of NORAD space surveillance sensors can be created. By placing the ground trace on this map, the time between sensor overflight can be computed using Kepler's time of flight equation (4, 185-186). This will give how much time the Soviets have to deploy a satellite and move it from a sensor's field of view. The ground trace will be placed on the Mercator projection map of the world, orbital revolution by revolution, so that all possible opportunities for an unobserved deployment can be examined.

Sensor Resolution. Two documents were used to provide data on sensor characteristics. They are the Space Command's technical memorandum "Ground-based Space and Missile Warning Characteristics" (U) (13) and the Science Applications, Inc. publication, "Space Surveillance Network Handbook" (U) (23). They provide data for range resolution and angular resolution for each sensor. Using approximate values for the slant range, it can be determined if the separation between shuttle and deployed satellite is inside or outside the "window of detectability" for that sensor. A probability of detection rating of "high" will be assigned for geometries that give angular separations that can be eaisly resolved by the radar; a rating of "low" will be given for angular separations much smaller than the angular resolution. A rating of "medium" will be given for situations that give angular separations that are nearly equal to the angular resolution. Range resolution is much easier to handle, since for the near-Earth orbits under analysis, separation will be detected if the range difference is more than the range resolution of the sensor. A probability rating of either "high", "medium" or "low" can be assigned if the shuttle-satellite range difference is larger, equal to, or less than the range resolution. Of course, a rating of "none" will be given if the shuttle and satellite do not rise above the sensor's horizon for any particular orbital revolution.

In the process of the analysis, the range and angular separation will be given in the geocentric inertial coordinate system, i.e., as seen from the center of the Earth. A change in these values will be needed to account for the way the radar sees the shuttle and satellite, i.e., the topocentric coordinate system. This change will be determined by the approximate slant range and elevation for each sensor.

At this point it is necessary to describe the geocentric inertial and topocentric coordinate systems. Each system can be described by defining the origin, fundamental plane and principle direction, and the displacements from these three basic components.

The origin of the geocentric inertial system is the center of the Earth, hence the word "geocentric". Any displacement from the origin is called a radius. The fundamental plane in this system is the celestial equator, which is constructed by extending the Earth's equator out into space. In fact, it is helpful to visualize a giant sphere surrounding the Earth, with the celestial equator co-planar with the Earth's equator. Displacement from the celestial equator is measured as a spherical angle called the declination. It is analogous to latitude in the geographic coordinate system, and the values run from 0° at the celestial equator to +90° at the North Celestial Pole to -90° at the South Celestial Pole. The principle direction is to a point called the First Point of Aries, or Aries for short, which is the ascending node of the Sun's apparent orbit (the ecliptic) on this celestial sphere. Displacement from Aries is called right ascension, and is measured eastwardly, from 0° to 360°. This celestial sphere is fixed in space in relation to the distant stars (assumed to be stationary); it does not revolve with the Earth, so it is inertial. See Figure 1.

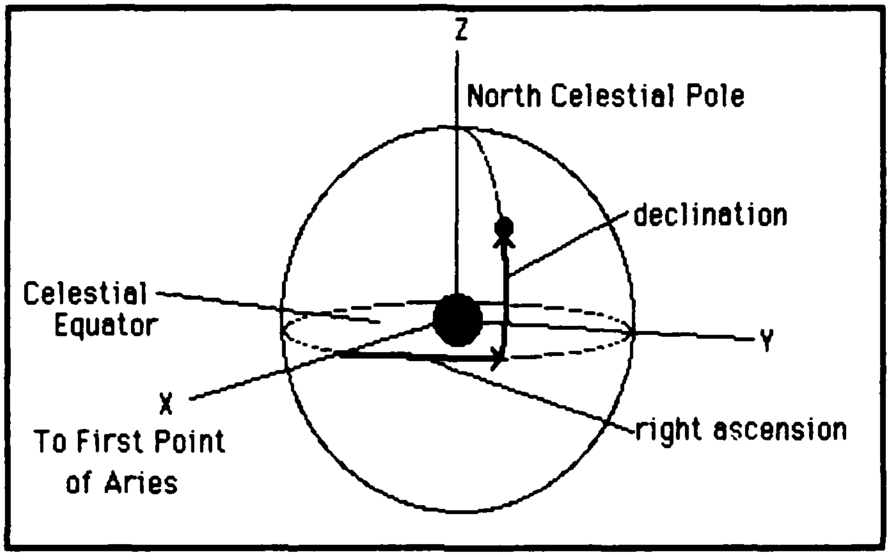

Figure 1. Geocentric Inertial System

The origin of the topocentric coordinate system is the observer, in this case the radar tracking station. Displacement from the observer is called the slant range. The fundamental plane is the observer's horizon, and displacement is the elevation angle. The values run from 0° to +90° (the zenith). The principle direction is True North, and the displacement is called the azimuth, measured clockwise from 0° to 360°. Since this coordinate system travels with the observer as the Earth revolves, it is not inertial. See Figure 2.

Soviet Satellites. Several Soviet surveillance satellites were possible candidates for analysis. The mission chosen was naval surveillance. There

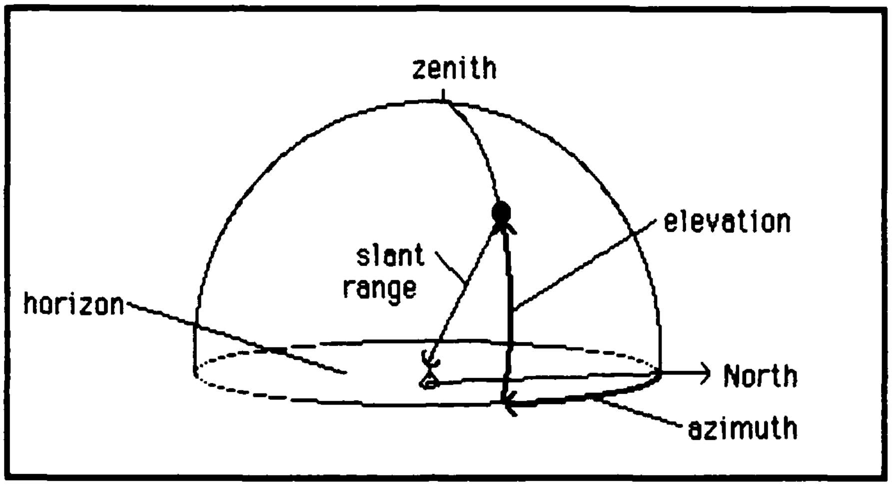

Figure 2. Topocentric System

two classes of naval reconnaissance satellites: Class A has an apogee height of 445 km and a perigee height of 435 km and an inclination of 65° (19, 105). Class B has an apogee of 275 km and a perigee of 260 km, and an orbital inclination of 65° (19, 120). Class A was chosen, because it is more likely the shuttle would be used to launch higher orbit satellites than lower orbit satellites.

Deployment process. The process for a Soviet shuttle attempting to hide a deployment will be different from that of a U.S. shuttle openly deploying a satellite. The general procedure used is to eject the satellite using a spring-loaded platform. Fifteen minutes after ejection, the shuttle performs a small maneuver burn that decreases the orbital period by approximately 6 seconds. Thirty minutes after that, the satellite is about 50 km from the shuttle and the satellite's rocket motor fires for injection into the new orbit (5). The Soviet shuttle would have the problem of leaving the satellite in the original orbit, where it would be easy to predict its location, if it used this method. Instead, the satellite should perform the maneuver to separate it from the shuttle, perhaps by using hydrazine thrusters. If the satellite is not observed by a NORAD sensor, there would be no indication by the shuttle's orbit that anything unusual has happened.

The orientation of the satellite is important, due to the need for the principle maneuver burn to change the orbit's semi-major axis and inclination. This orientation can be determined by examining the geometry of the initial velocity vector, the final velocity vector and the "delta-v", i.e., the velocity change vector. This also gives the pitch angle, or how the satellite must be rotated from pointing in the initial velocity vector direction. Since inclination changes are necessary, the most efficient point for the maneuver burn is at an ascending or descending node. Also, since maximum separation from the hydrazine thruster burn will take place half an orbital revolution later, this initial delta-v must take place at a node.

Earlier, a separation distance of 50 km between the U.S. shuttle and satellite was noted. This distance provides a measure of safety for the shuttle, to prevent rocket engine exhaust from impinging on and possibly damaging the shuttle, and in case the rocket engine explodes, it is less likely that the shuttle will be struck by debris. The Soviet shuttle would reasonably require a separation of the same order of magnitude.

When the hydrazine thrusters fire, the satellite will be quite close to the shuttle, but at that point the orbital parameters of the satellite will be updated. During the time between the hydrozine thruster burn and the main rocket engine burn, the map will be checked to see if any NORAD sensor would be able to view the shuttle and the probability of viewing the satellite. At the time of the main rocket engine firing, the orbital elements will again be updated, and again the map will be checked to determine when the next NORAD sensor will be able to track the shuttle. The separation distance and angular displacement will be determined, thereby leading to the probability of detection rating.

From this analysis, it can be determined how probable it would be for the U.S.S.R. to hide satellite deployment from NORAD ground-based space surveillance sensors.

Decision Rules

The decision rules listed below are used as an aid to determine the probability of the radar site detecting the deployed satellite. Detection depends upon the radar characteristics, the satellite-shuttle separation distance, and the angle of elevation the radar has when viewing the spacecraft.

1. Satellites with an estimated maximun elevation of 5° or less have a low or no probability of being detected, as well as the shuttle-satellite pair having a range difference or angular separation smaller than the radar's limiting resolution.

2. If the shuttle-satellite pair has a range difference and angular separation approximately equal to the radar's limiting resolution, then there is a medium probability the satellite will be detected.

3. If the shuttle-satellite pair has a range difference or angular separation greater than the radar's limiting resolution, then there is a high probability the satellite will be detected.

4. Angular separation is based on geocentric coordinates of right ascension and declination, but sensors observe in the topocentric coordinates of azimuth and elevation. Therefore, angular separation can be foreshortened (appear to be smaller due to the site observing the spacecraft from the side) at elevations less than 90°, and the degree of foreshortening

also depends on the relative angular position of the shuttle and satellite to the observing sensor. A worst case condition will be assumed, so the foreshortening will depend solely on the elevation angle. Also, since the radar is much closer to the satellites than the Earth's center, the angular separation may be larger than calculated. These two conflicting conditions are shown in Figures 3 and 4, with accompanying equations.

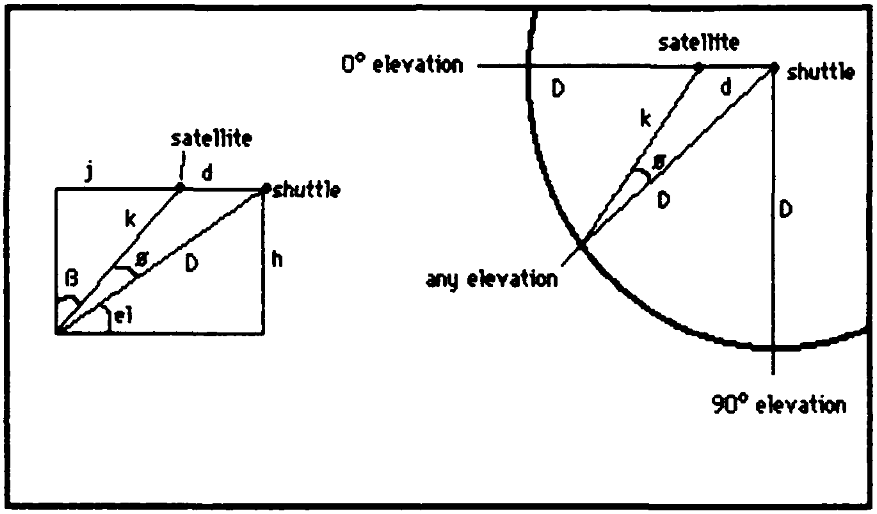

Figure 3. Apparent Angular Separation

For the above illustration, angle el is the elevation angle as viewed by the sensor, angle ø is the apparent angular separation, and angle ß is the remaining complementary angle. Distance D is the sensor-shuttle slant range, d is the shuttle-satellite distance, k is the sensor-satellite distance and h and j are convenient sides to keep the trigonometry to simple right triangles. Since D, d and el are known, h and j are solved for by $h = D \sin el$ and $j = (D \cos el) - d$. Then solve for k by $k = [D^2 + d^2 - 2 D d \cos (el)]^{1/2}$. Solve for ø by $ø = \arccos [(D^2 + k^2 - d^2) / (2 D k)]$, and D - k is the range difference as seen by the sensor.

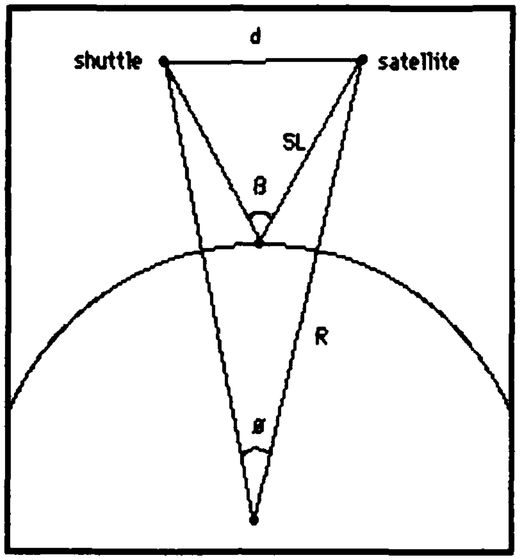

Figure 4. Relation Between Geocentric and Topocentric Separation Angle

For Figure 4, ø is the geocentric separation angle and ß is the topocentric separation angle. R is the distance from the Earth's center to the shuttle or satellite (assumed to be the same in this simple illustrative case), and SL is the slant range from the sensor to the shuttle or satellite. The angle ø can be found by $\sin(ø / 2) = (d / 2) / R$, while the angle ß is found by $\sin(ß / 2) = (d / 2) / SL$.

5. As seen from a topocentric site, range separation can be seen as an angular separation, which can be calculated with the slant range distance to the shuttle and the distance of the satellite from the shuttle. See Figure 5. Taking Rules 2 and 3 together, the larger angular separation angle calculated will be the one used to determine detection probability. Also, the range separation as seen by the sensor can be figured from the slant range distance and elevation angle.

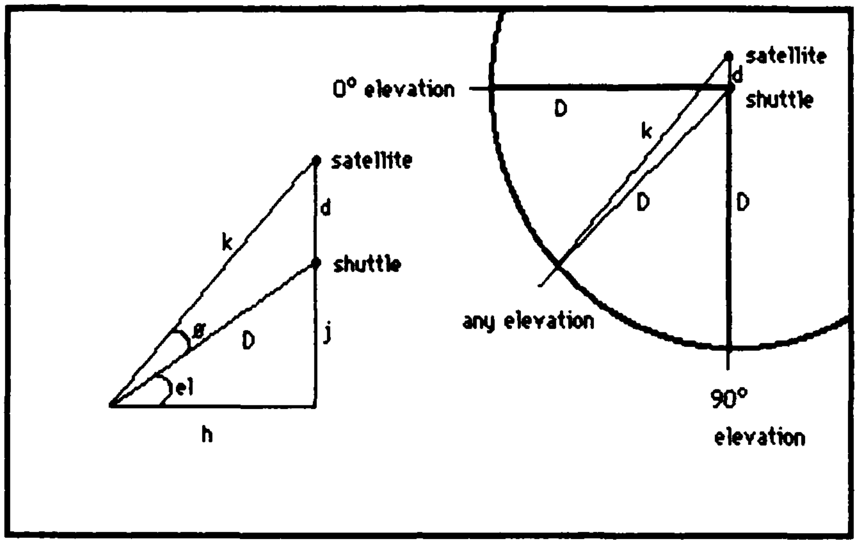

Figure 5. Range Difference Appears As
Angular Separation

In Figure 5, angle el is the elevation angle, angle ø is the apparent angular separation, distance D is the sensor-shuttle slant range and d is the shuttle-satellite separation distance. Sides h and j are convenient sides to keep the trigonometry to simple right triangles, while side k is the sensor-satellite distance. Since D, d, and el are known, solve for j by $j = D \sin el$. Then solve for h by $h = D \cos el$, and then solve for angle ø with $ø = \arctan[(d + j) / h] - el$. Find distance k by $k = (d + j) / \sin(ø + el)$. The range difference as seen by the sensor is then $D - k$.

6. Maximum elevation angle will be estimated from how much the ground trace cuts into the sensor surveillance area on the map. Slant range is then determined from this angle. See Figure 6 and Table I for numerical values.

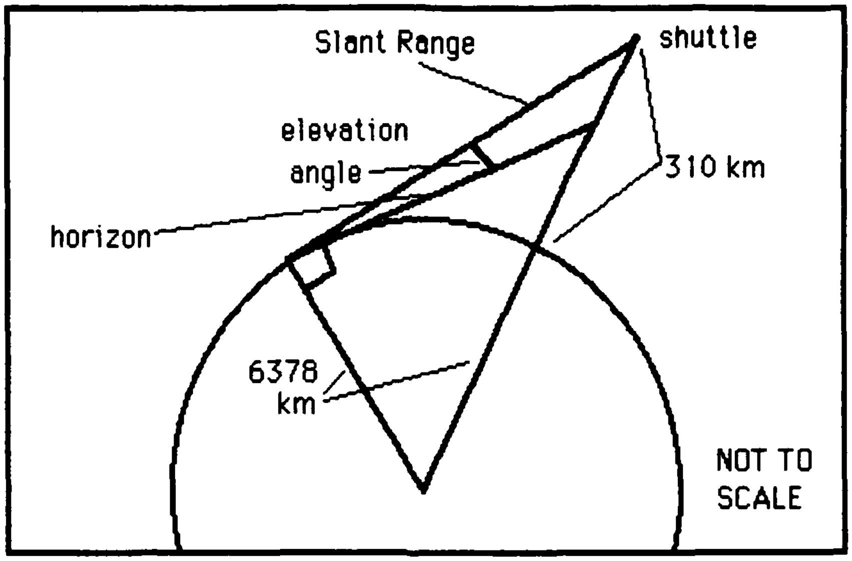

Figure 6. Slant Range and Elevation

Table I

Elevation and Slant Range Values

Elevation	Slant Range in km
0°	2012.58
5°	1532.05
10°	1189.66
15°	952.22
20°	786.59
25°	668.46
30°	581.97
35°	517.06
40°	467.36
45°	428.69
50°	398.28
55°	374.23
60°	355.23
65°	340.34
70°	328.89
75°	320.40
80°	314.56
85°	311.13
90°	310.00

The values in Table I for slant range were based on the elevation value, and calculated using the following formula:

$$SL = (6688 \text{ km}) \cos \{el + \arcsin [(6378 \text{ km} / 6688 \text{ km}) \cos el] \} / \cos (el)$$

where SL is the slant range and el is the elevation angle. Euclidean geometry was used to determine this formula, employing angle reduction formulas.

Chapter Three lists the sensor locations and capabilities, describes the Soviet shuttle's orbital parameters at an ascending node and how the satellite deployment velocities are computed. Next is a listing of opportunities for the NORAD radars to observe the deployed satellite for each of the first thirty orbits, assuming the deployment takes place at that revolution's ascending node. Finally, a table lists for each revolution which sensors will see the shuttle-satellite pair, the worst-case relative range separation and relative angular separation for each of the three deployment directions, and the probability of detection.

Chapter Three

Findings

Chapter Overview

This chapter will present the probabilities of the NORAD radars detecting both the Soviet shuttle and deployed satellite and how the probabilities are determined. This is followed by a section on the shuttle's orbital parameters, which provide the information necessary for determining the additional velocity applied to the satellite for deployment. Thus the satellite separation velocity during the deployment phase can be computed. Deployment is to be initiated at an ascending or descending node, and not every orbit can be used to covertly deploy the satellite. The shuttle will pass over various NORAD sensors at different parts of its orbit, and each orbital pass will overfly different radars. This provides times of opportunities for the sensors to observe the shuttle at various elevations and slant ranges. Finally, the probabilities of detection by each sensor for each of the first thirty orbits of the shuttle are determined.

Sensors

Space Command / NORAD has many space surveillance radar sites located throughout the world. Figure 7 is a Mercator projection map, with the sites used in this thesis' analysis marked by a cross. They are numbered one through thirteen, which corresponds to the list of site names and information in Table II. The circles on the map represent the volume of space observed by the radar, as it pertains to tracking a spacecraft in an orbit with a 310 km altitude. Note that in Table II, some data is listed as classified. Any time this information is needed for determining a probability of detectior., the original, classifed documents are referenced, and the probability of detection is then decided.

Soviet Shuttle Orbital Parameters

The orbit traces for the first thirty orbital revolutions of the Soviet shuttle are in Appendix A. NORAD uses the convention of calling the ascending node of an orbit its start, and that convention is followed here. The Keplerian element set used to generate the orbit trace has a semi-major axis of 6688.145 km, eccentricity of 0.00°, inclination of 51.62°, argument of perigee of 0.00° (perigee is placed at the ascending node because a perfectly circular orbit has no one point that is closest to the Earth), right ascension of the ascending node of 180.00°, and epoch time at ascending node of 1200 hrs. (The last two are arbitrary values; they have no bearing on the final analysis and are dependent upon day of the year and time of day of launch.) This orbit has a period of 1.51205 hours (1 hour, 30 minutes, 43.4 seconds), and a constant orbital velocity of 7.71998 km/sec. This element set is translated into position and velocity vectors using an algorithm in Bate, Mueller, and White (4, 71-83). The results are shown in Table III where "r" is the position vector components in km, "v" is the velocity vector components in km/sec, and "H" is the angular momentum vector components in km^2/sec. The word "sub" is a shortening of "subscript"; the vectors are given as components in the geocentric inertial coordinate system. The word "unit" signifies the value listed is a component for the unit vector in the "r", "v" or "H" direction. The program listing in Microsoft® Basic 2.0 for the Apple® Macintosh™ is in Appendix B.

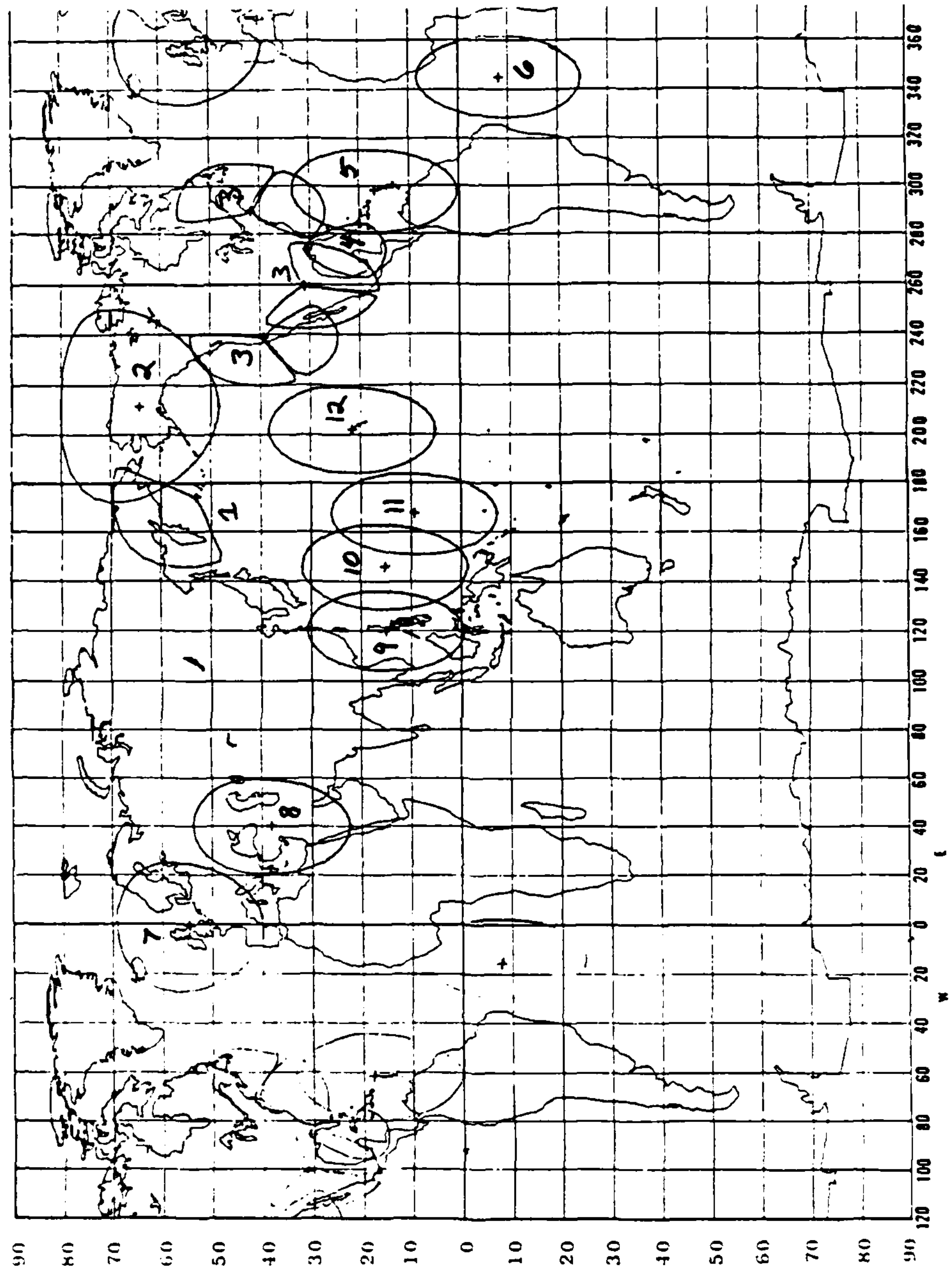

Figure 7. Sensor Locations

Table II. Sensor Capabilities

Sensor name	Range resolution	Beam width	Reference
1. COBRA DANE AN/FPS-108	24 - 122 meters	2.2°	(23, 25)
2. Clear AFS			
AN/FPS-92	classified	2.0°	(23, 21)
AN/FPS-50	large†	1.0°	(13, 1-8, 9)
3. PAVE PAWS AN/FPS-115	190 meters	2.18°	(23, 49; 13, 1-28, 29)
4. Eglin AFB AN/FPS-85	classified	0.8°	(23, 45)
5. Antigua Is. AN/FPQ-14	750 meters	0.28°	(23, 35)
6. Ascension Is. AN/FPQ-15	1500 meters	0.28°	(23, 37)
7. Fylingdales AN/FPS-49	large†	2.2°	(23, 25)
8. Priniclik			
AN/FPS-79	classified	1.9°	(23, 27)
AN/FPS-17M	3.597 km	1.0°	(13, 2-10, 11)
9. San Miguel AN/GPS-10	classified	2.0°	(23, 33; 13, 2-15,16)
10. Saipan††	(750 meters)	(0.28°)	
11. ALTAIR	15 meters	1.1°	(23, 67)
12. Kaena Pt AN/FPQ-14	45.72 meters	0.4°	(23, 39)

† actual value is classified
†† projected radar site; sensor data is based on the AN/FPQ-14 on Antigua

Table III. Initial Shuttle Vectors		
Vector Magnitudes		
r vector	v vector	H vector
r = 6688.14500	v = 7.71998	H = 51,632.37879
r sub x = -6688.14500	v sub x = 0.00	H sub x = 0.00
r sub y = 0.00	v sub y = -4.79314	H sub y = 40,475.14998
r sub z = 0.00	v sub z = 6.05178	H sub z = 32,057.21093
unit r sub x = -1.00	unit v sub x = 0.00	unit H sub x = 0.00
unit r sub y = 0.00	unit v sub y = -0.62087	unit H sub y = 0.78391
unit r sub z = 0.00	unit v sub z = 0.78391	unit H sub z = 0.62087

Computation of Satellite Deployment Velocities

The initial satellite deployment phase is where the satellite is released from the payload bay and fires its hydrazine thrusters to move away from the shuttle. The satellite may move in any direction, but the three shuttle-centered principle directions are the radius vector direction, the velocity vector direction, and the angular momentum vector direction, which is mutually perpendicular to the first two. The additional velocity imparted to the satellite so that it can be deployed along one of these three directions can be found by multiplying the unit vectors in the preferred direction of r, v, or H by some arbitrary velocity. This can then be added vectorally to the given velocity vector of the shuttle, to give the new velocity vector of the satellite. For example, the satellite will move 5 m/sec away from the shuttle along the velocity vector. Therefore, multiply 0.005 (to convert to km/sec) by 0.00, -0.62087, and 0.78391 to get 0.00, -0.00310, and 0.00392, and then add to the shuttle's velocity vector to get v sub x = 0.00, v sub y = -4.79624, and v sub z = 6.05569. With this new orbital element set, allow the satellite to fly from the shuttle for one half of a revolution, and see how far away the satellite is from the shuttle at the end at this time. The satellite should be about 50 km or more from the shuttle for safety considerations, so the arbitrary velocity chosen must give this distance half an orbit later. If the distance is too small, increase the velocity and try again; if it is too large, decrease it. This trial-and-error method is unsophisticated, but it works, and works for all three vector directions.

If the satellite is deployed along the radius vector, it must move along this vector at a velocity of 15 meters/second, so that the satellite-shuttle separation distance one half revolution away is 52.1 km, thereby meeting the safety requirement. As seen from the Earth's center, the range difference between the shuttle and the satellite is only 101 meters, and the angular separation is 0.42°. This measure of range and angular separation will be referred to as the true range distance and true angular separation, which may be different from how the radar site sees the shuttle and satellite (which are listed in Table V). These values were found by translating the position and velocity vectors of the deployed satellite into Keplerian elements (4, 61-63) and then into a position of right ascension and declination after a time elapse of one half a period (4, 182-188). (Programs are listed in Appendix B.)

If the additional velocity used in deployment is along the velocity vector, it need move only 5 meters/second to be 44.3 km away from the shuttle half a period later, so only a little bit more is needed to have a 50 km separation. A 5 meters/ second vector addition will give a true range distance of 17.6 km, and a true angular separation of 0.35°.

If the additional velocity used in the satellite deployment is along the angular momentum vector, it will need to move at a speed of 300 meters/

second to give a separation distance of 51.6 km. This is a huge increase in comparison to the first two deployment schemes, and would require a long burn time for the hydrazine thrusters. True angular separation will be 0.41°. True range distance is 20.23 km.

Times of Opportunities

Figure 8 is an example of an orbital pass map. The satellite moves from left to right, and at the ascending node it begins a new revolution. The orbit revolution number is written near the ascending node. Note the sinusoidal line; it is called the ground trace. It is the set of points on the Earth over which the satellite passes in the orbit. From the orbital pass maps in Appendix A, there are numerous times when the shuttle and newly deployed satellite travel through a volume of space that is being monitored by a NORAD radar station. The problem to be solved at this point is the likelihood the radar can distinquish the two spacecraft.

Table IV lists the sensors that can observe the shuttle and satellite for each of the thirty orbital revolutions. The true anomaly listed is the value for that particular orbit when the satellite reaches the closest approach to the radar site; the maximum elevation listed is the estimated maximum elevation observed by that site. The closest approach point was chosen because it is here that the sensor has the best opportunity to discern if there are one or two spacecraft in orbit. The range values are taken from Table I.

It is assumed the shuttle will attempt a deployment at all nodes; the true anomaly listed in Table IV is the number of degrees from that orbit's ascending node. By multiplying this angle by 0.004200143 hours / degree, the time of flight from ascending node is obtained, and this is used to

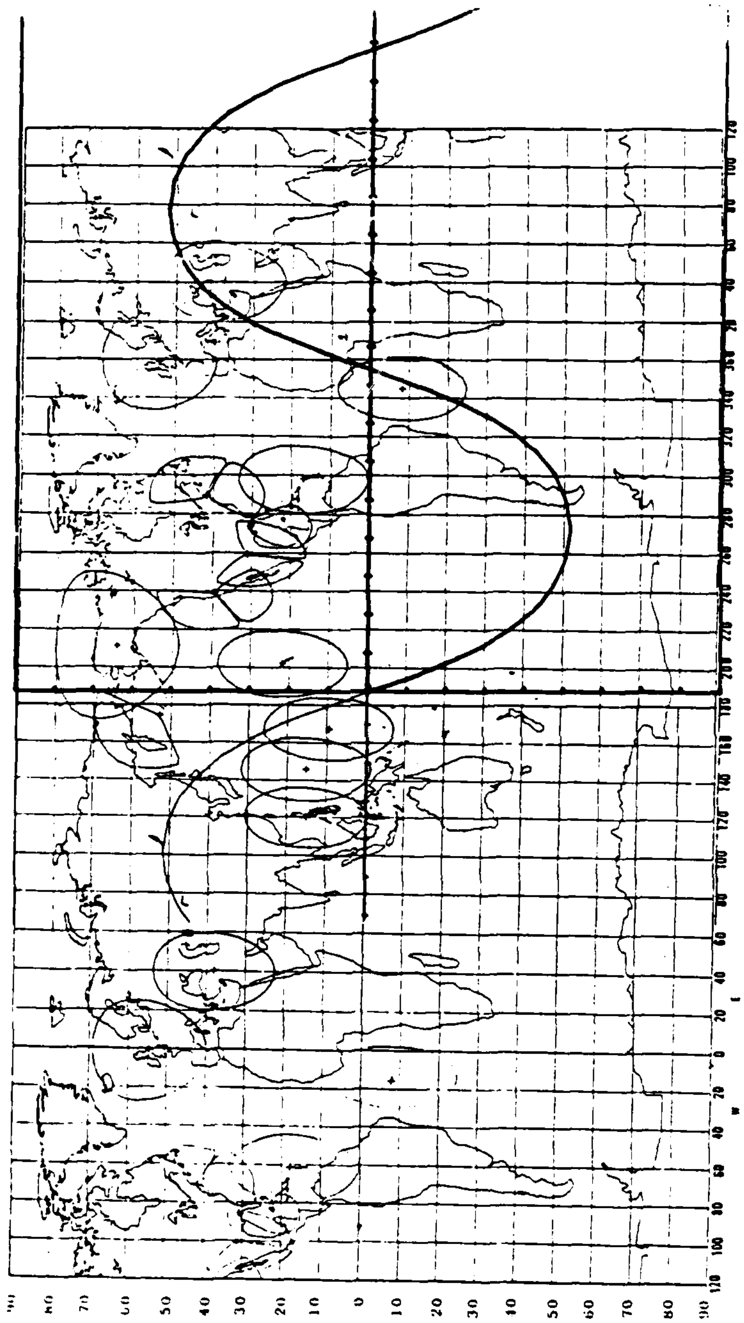

Figure 8. Orbital Pass Map

calculate how far away the satellite is from the shuttle, the true range, and the true angular separation, for all three deployment directions. Then assume the worst possible viewing geometry (see Figures 3 and 5) to get the apparent range difference and the apparent angular separation. Finally, compare these last two values to Table II, and determine the probability of detection. These are listed in Table V.

For example, refer to Revolution 4 in Table IV. The sites at Antigua, Fylingdales and Pirinclik observe the shuttle-satellite pair at the shuttle's true anomaly values of 30°, 90°, and 119°, respectively. At 30° past the ascending node, the satellite has an apparent range difference of 1,174 meters and an apparent angular separation of 0.38°, if deployed along the r vector. Since the Antigua radar has a range resolution of 750 meters and an angular separation of 0.28° (the beamwidth), the radar can easily detect the two distinct objects, so the probability of detection rating is "high". However, if the satellite is deployed along the v vector, the range difference is only 631 meters and the angular separation is 0.07°. Therefore, the radar cannot distinguish the two objects, and the probability rating is "low". This method is applied to all sensors, for all three deployment vectors. The final step is to determine the probability of detection for the entire half orbit. The highest probability rating per one-half revolution for any one deployment vector is the probability assigned for that one-half revolution. So even though Antigua and Fylingdales both have a "low" rating for deployment along the v vector in Revolution 4, the "high" probability rating at Pirinclik gives a "high" probability of detection for the half revolution.

Some of the sensors listed in Tables IV and V are abbreviated; "PPW" stands for PAVE PAWS West, "PPE" stands for PAVE PAWS East, and "PPSW" stands for PAVE PAWS SouthWest.

Table IV. Times of Opportunities

Revolution	sensor	true anomaly	max. elevation	range (km)
1	Pirinclik	64°	50°	398.28
	Saipan	156°	80°	314.56
	ALTAIR	169°	45°	428.69
2	Pirinclik	81°	10°	1189.66
	San Miguel	157°	80°	314.56
	Saipan	162°	5°	1532.05
3	Antigua	22°	5°	1532.05
	Fylingdales	76°	60°	355.23
	Pirinclik	100°	25°	668.46
4	Antigua	30°	70°	328.89
	Fylingdales	90°	80°	314.56
	Pirinclik	119°	75°	320.40
5	Eglin	45°	45°	428.69
	PPE	58°	70°	328.89
	Fylingdales	100°	60°	355.23
	Pirinclik	129°	50°	398.28
6	PPSW	48°	90°	310.00
	PPE	71°	45°	428.69
	Fylingdales	112°	25°	668.46
7	PPW	57°	80°	314.56
	PPE	90°	30°	581.97
8	Kaena Pt.	34°	90°	310.00
	PPW	71°	45°	428.69
	PPE	107°	50°	398.28
	Ascension	190°	45°	428.69
9	ALTAIR	14°	85°	311.13
	PPW	90°	10°	1189.66
	PPE	121°	80°	314.56
	Antigua	149°	30°	581.97
	Ascension	193°	5°	1532.05

Table IV. Times of Opportunities, continued

Revolution	sensor	true anomaly	max. elevation	range (km)
10	Saipan	23°	85°	311.13
	Clear	87°	20°	786.59
	PPW	116°	25°	668.46
11	San Miguel	21°	90°	310.00
	Clear	99°	5°	1532.05
	PPW	122°	90°	310.00
	PPSW	139°	55°	374.23
12	COBRA DANE	92°	80°	314.56
	PPW	133°	5°	1532.05
13	Kaena Pt.	144°	75°	320.40
14	Kaena Pt.	153°	5°	1532.05
	Ascension	345°	10°	1189.66
15	Pirinclik	58°	90°	310.00
	Saipan	154°	20°	786.59
	ALTAIR	168°	90°	310.00
	Ascension	349°	45°	428.69
16	Pirinclik	71°	25°	668.46
	ALTAIR	153°	5°	1532.05
	Saipan	160°	60°	355.23
17	Fylingdales	70°	40°	467.36
	Pirinclik	90°	10°	1189.66
	San Miguel	160°	40°	467.36
18	Antigua	25°	90°	310.00
	Fylingdales	82°	75°	320.40
	Pirinclik	113°	40°	467.36
19	Eglin	39°	30°	581.97
	PPE	55°	45°	428.69
	Fylingdales	95°	80°	314.56
	Pirinclik	124°	85°	311.13

Table IV. Times of Opportunities, continued

Revolution	sensor	true anomaly	max. elevation	range (km)
20	PPSW	44°	85°	311.13
	PPE	67°	75°	320.40
	Fylingdales	109°	40°	467.36
21	PPW	51°	45°	428.69
	PPSW	54°	10°	1189.66
	PPE	83°	30°	581.97
22	Kaena Pt.	29°	60°	355.23
	PPW	62°	60°	355.23
	PPE	97°	40°	467.36
23	ALTAIR	11°	80°	314.56
	Kaena Pt.	40°	15°	952.22
	PPW	78°	10°	1189.66
	PPE	113°	85°	311.13
	Ascension	192°	85°	311.13
24	Saipan	20°	80°	314.56
	Clear	82°	10°	1189.66
	PPW	98°	10°	1189.66
	PPE	130°	15°	952.22
	Antigua	155°	90°	310.00
25	San Miguel	20°	50°	398.28
	Saipan	28°	5°	1532.05
	Clear	94°	15°	952.22
	PPW	113°	50°	398.28
	PPSW	134°	90°	310.00
	Eglin	140°	45°	428.69
26	COBRA DANE	90°	90°	310.00
	PPW	128°	40°	467.36
27	COBRA DANE	96°	40°	467.36
	Kaena Pt.	140°	30°	581.97
28	Kaena Pt.	151°	55°	374.23

Table IV. Times of Opportunities, continued

Revolution	sensor	true anomaly	max. elevation	range (km)
29	Pirinclik	53°	80°	314.56
	ALTAIR	165°	55°	374.23
	Ascension	348°	90°	310.00
30	Pirinclik	68°	45°	428.69
	Saipan	158°	85°	311.13

Table V. Probability of Detection

Revolution Node	Sensor	r vector	v vector	H vector
		apparent range difference (meters) apparent angular separation (degrees) probability of detection		
1, A.N.	Pirinclik	9,023 1.06 high	679 0.17 high	4,360 0.52 high
	Saipan	4,741 0.17 high	3,659 0.50 high	348 0.58 high
	ALTAIR	1,827 0.24 high	12,322 1.58 high	14,391 1.83 high
D.N.	not seen			
2, A.N.	Pirinclik	2,299 0.18 high	1,237 1.05 high	1,508 0.40 high
	San Miguel	4,744 0.16 high	3,702 0.50 high	307 0.58 high
	Saipan	364 0.15 low	1,567 0.10 high	1,844 0.31 high
D.N.	not seen			
3, A.N.	Antigua	432 0.006 low	55 0.005 low	64 0.03 low
	Fylingdales	9,415 0.99 low	212 0.06 low	6,648 0.61 low
	Pirinclik	5,524 0.99 high	4,360 0.20 high	5,092 0.91 high
D.N.	not seen			

Table V. Probability of Detection, continued

Revolution Node	Sensor	r vector	v vector	H vector
		apparent range difference (meters)		
		apparent angular separation (degrees)		
		probability of detection		
4, A.N.	Antigua	1,174	631	1,271
		0.38	0.07	0.08
		high	low	high
	Fylingdales	3,455	520	9.946
		0.40	0.27	0.31
		low	low	low
	Pirinclik	7,753	2,852	14,501
		0.51	0.57	0.66
		high	high	high
D.N.	not seen			
5, A.N.	Eglin	5,342	1,446	2,096
		0.73	0.19	0.28
		high	high	high
	PPE	3,970	523	1,566
		0.64	0.24	0.28
		high	high	high
	Fylingdales	11,169	2,770	10,308
		1.0	0.79	0.93
		low	low	low
	Pirinclik	7,840	9,941	12,737
		0.92	1.27	1.47
		high	high	high
D.N.	not seen			
6, A.N.	PPSW	119	6	3,341
		0.00	0.00	0.00
		low	low	high
	PPE	8,783	198	4,841
		1.14	0.55	0.64
		high	med	low
	Fylingdales	5,201	5,119	5,981
		0.93	0.34	1.07
		low	low	low
D.N.	not seen			

Table V. Probability of Detection, continued

Revolution Node	Sensor	r vector	v vector	H vector
		apparent range difference (meters) apparent angular separation (degrees) probability of detection		
7, A.N.	PPW	1,835 0.33 high	274 0.12 high	4,529 0.14 high
	PPE	6,618 1.10 high	2,666 0.15 high	5,112 0.85 high
D.N.	not seen			
8, A.N.	Kaena Pt.	32 0.00 low	1,482 0.00 high	1,726 0.00 high
	PPW	8,783 1.14 high	198 0.03 med	4,841 0.64 high
	PPE	9,631 1.13 high	4,895 0.86 high	10,080 1.18 high
D.N.	Ascension	279 0.21 low	93 0.01 low	108 0.01 low
9, A.N.	ALTAIR	3,132 0.14 high	8,694 0.004 high	299 0.005 high
	PPW	2,330 0.22 high	1,535 0.03 high	1,794 0.48 high
	PPE	4,375 0.35 high	1,937 0.40 high	15,073 0.46 high
	Antigua	3,419 0.57 high	8,214 1.27 high	9,602 1.57 high

Table V. Probability of Detection, continued

Revolution Node	Sensor	r vector	v vector	H vector
		apparent range difference (meters) apparent angular separation (degrees) probability of detection		
9, D.N.	Ascension	258	19	26
		0.002	0.003	0.01
		low	low	low
10, A.N.	Saipan	173	132	800
		0.38	0.01	0.01
		low	low	low
	Clear	4,541	2,279	3,323
		0.63	0.06	0.65
		high	high	high
	PPW	5,042	5,361	6,265
		0.90	0.39	1.11
		high	high	high
D.N.	not seen			
11, A.N.	San Miguel	4,657	576	671
		0.00	0.00	0.00
		high	high	high
	Clear	1,175	906	1,061
		0.10	0.02	0.43
		high	high	high
	PPW	2,536	270	15,445
		0.00	0.00	0.00
		high	high	high
	PPSW	7,079	11,161	14,648
		0.74	1.29	1.50
		high	high	high
D.N.	not seen			
12, A.N.	COBRA DANE	3,537	596	10,293
		0.40	0.28	0.32
		high	high	high
	PPW	864	1,339	1,573
		0.15	0.06	0.63
		high	high	high

Table V. Probability of Detection, continued

Revolution Node	Sensor	r vector	v vector	H vector
		apparent range difference (meters) apparent angular separation (degrees) probability of detection		
12, D.N.	not seen			
13, A.N.	Kaena Pt.	7,464	5,059	17,680
		0.35	0.69	0.80
		high	high	high
D.N.	not seen			
14, A.N.	Kaena Pt.	534	1,516	1,783
		0.17	0.09	0.43
		high	high	high
D.N.	Ascension	606	3,079	3,611
		0.16	0.28	0.70
		low	high	high
15, A.N.	Pirinclik	240	4	4,746
		0.00	0.00	0.00
		low	low	high
	Saipan	1,998	5,781	6,766
		0.40	0.70	1.30
		high	high	high
	ALTAIR	2,801	1,904	7,341
		0.00	0.00	0.00
		high	high	high
D.N.	Ascension	1,827	12,322	14,391
		0.24	1.58	1.83
		high	high	high
16, A.N.	Pirinclik	5,290	253	2,906
		0.65	1.01	0.53
		high	low	high
	ALTAIR	534	1,516	1,783
		0.17	0.09	0.43
		high	high	high

Table V. Probability of Detection, continued

Revolution Node	Sensor	r vector	v vector	H vector
		apparent range difference (meters) apparent angular separation (degrees) probability of detection		
16, A.N.	Saipan	3,939 0.36 high	14,134 1.30 high	17,103 1.51 high
D.N.	not seen			
17, A.N.	Fylingdales	7,949 1.13 low	310 0.03 low	4,297 0.62 low
	Pirinclik	2,330 0.22 high	1,535 0.03 high	1,794 0.48 high
	San Miguel	2,931 0.42 high	10,985 1.54 high	12,833 1.79 high
D.N.	not seen			
18, A.N.	Antigua	5,492 0.00 high	4 0.00 low	946 0.00 high
	Fylingdales	5,042 0.57 low	369 0.25 low	8,401 0.39 low
	Pirinclik	7,809 1.11 high	7,359 0.77 high	9,145 1.29 high
D.N.	not seen			
19, A.N.	Eglin	4,132 0.29 high	968 0.10 high	1,128 0.19 high
	PPE	7,595 0.99 high	1,213 0.16 high	3,055 0.40 high

Table V. Probability of Detection, continued

Revolution Node	Sensor	r vector	v vector	H vector
		apparent range difference (meters) apparent angular separation (degrees) probability of detection		
19, A.N.	Fylingdales	3,655	715	10,813
		0.39	0.29	0.34
		low	low	low
	Pirinclik	895	895	15,684
		0.17	0.21	0.24
		high	high	high
D.N.	not seen			
20, A.N.	PPSW	550	172	2,823
		0.14	0.04	0.05
		high	med	high
	PPE	3,723	194	5,945
		0.53	0.13	0.28
		high	med	high
	Fylingdales	8,020	6,345	8,711
		1.14	0.66	1.23
		low	low	low
D.N.	not seen			
21, A.N.	PPW	6,748	1,340	2,655
		0.92	0.18	0.35
		high	high	high
	PPSW	1,871	625	730
		0.50	0.01	0.20
		high	high	high
	PPE	6,565	1,407	4,483
		1.09	0.08	0.75
		high	high	high
D.N.	not seen			
22, A.N.	Kaena Pt.	1,617	908	1,097
		0.46	0.09	0.10
		high	high	high

Table V. Probability of Detection, continued

Revolution Node	Sensor	r vector	v vector	H vector
		apparent range difference (meters) apparent angular separation (degrees) probability of detection		
22, A.N.	PPW	6,680	616	4,648
		0.90	0.17	0.43
		high	high	high
	PPE	8,414	3,663	7,358
		1.19	0.38	1.05
		high	high	high
D.N.	not seen			
23, A.N.	ALTAIR	2,442	140	183
		0.08	0.005	0.006
		high	high	high
	Kaena Pt.	2,196	527	614
		0.10	0.03	0.14
		high	high	high
	PPW	2,276	730	1,415
		0.17	0.006	0.38
		high	high	high
	PPE	1,054	693	13,988
		0.19	0.19	0.22
		high	high	high
D.N.	Ascension	2,692	76	17
		0.04	.003	0.004
		high	low	low
24, A.N.	Saipan	268	238	600
		0.14	0.02	0.02
		low	low	low
	Clear	2,305	1,318	1,540
		0.19	0.01	0.41
		high	high	high
	PPW	2,308	1,753	2,051
		0.25	0.04	0.54
		high	high	high

Table V. Probability of Detection, continued

Revolution Node	Sensor	r vector	v vector	H vector
		apparent range difference (meters) apparent angular separation (degrees) probability of detection		
24, A.N.	PPE	2,643	3,783	4,427
		0.58	0.26	0.96
		high	high	high
	Antigua	3,940	1,241	19,259
		0.00	0.00	0.00
		high	high	high
D.N.	not seen			
25, A.N.	San Miguel	1,005	401	467
		0.17	0.05	0.06
		high	high	high
	Saipan	544	88	103
		0.01	0.006	0.04
		low	low	low
	Clear	3,445	2,441	2,852
		0.44	0.06	0.63
		high	high	high
	PPW	9,274	6,140	10,854
		1.09	1.08	1.26
		high	high	high
	PPSW	3,111	516	17,111
		0.00	0.00	0.00
		high	high	high
	Eglin	6,003	10,956	12,791
		0.79	1.41	1.64
		high	high	high
D.N.	not seen			
26, A.N.	COBRA DANE	1,084	15	10,094
		0.00	0.00	0.00
		high	low	high
	PPW	6,690	9,119	10,648
		0.95	1.24	1.50
		high	high	high
D.N.	not seen			

Table V. Probability of Detection, continued

Revolution Node	Sensor	r vector	v vector	H vector
		apparent range difference (meters) apparent angular separation (degrees) probability of detection		
27, A.N.	COBRA DANE	8,431	3,464	7,244
		1.20	0.36	1.03
		high	high	high
	Kaena Pt.	4,162	7,802	9,119
		2.42	1.04	1.50
		high	high	high
D.N.	not seen			
28, A.N.	Kaena Pt.	5,251	13,424	15,663
		0.55	1.38	1.60
		high	high	high
D.N.	not seen			
29, A.N.	Pirinclik	1,629	310	3,960
		0.32	0.11	0.13
		high	low	high
	ALTAIR	2,840	14,090	16,442
		0.30	1.44	1.67
		high	high	high
D.N.	Ascension	2,800	1,904	7,341
		0.00	0.00	0.00
		high	high	high
30, A.N.	Pirinclik	8,610	454	4,488
		1.12	0.06	0.59
		high	med	high
	Saipan	331	1,176	8,133
		0.08	0.25	0.29
		low	high	high
D.N.	not seen			

Probabilities for Hidden Deployments

To summarize the findings reported in Table V, there is generally a high probability of the NORAD sensors detecting a deployment from a Soviet shuttle, if the radar has the opportunity to view the shuttle. Only a few times are there medium or low probabilities of detection. Unfortunately, there are many times that there is no radar available to track and observe the shuttle. This occurs in the Southern Hemisphere, where there is only the Ascension Island radar, and it covers only a small portion of the South Atlantic.

There is a high probability of detection by one radar or another for the following portions of the orbital revolutions: Revs 1 - 5, ascending node to descending node portion (abbreviated AN), Rev 6 AN r and H vector deployments, Revs 7 - 14 AN, Rev 14 descending node to ascending node portion (abbreviated DN) v and H vector deployments, Rev 15 AN and DN, Revs 16 - 23 AN, Rev 23 DN r vector deployment, Revs 24 - 28 AN, Rev 29 AN and DN, and Rev 30 AN.

There is only a medium chance of detection for Rev 6 AN v vector deployment and Rev 20 AN v vector deployment. There is a low probability of detection for Revs 8 and 9 DN, Rev 14 DN r vector deployment, and Rev 23 DN v and H vector deployments.

The most disturbing fact revealed by Table V is that the vast majority of the descending node portion of the orbits are unobserved. These are Revs 1 - 7 DN, 10 - 13 DN, 16 - 22 DN, 24 - 28 DN and 30 DN, which is 80% of the first thirty revolutions.

Chapter Four will examine the case of a main engine firing to place the deployed satellite into a transfer orbit and the subsequent detection probability for the next sensor to view it. It will list the best deployment times noted in the first thirty revolutions, and present limitations in this study and recommendations for further study.

Chapter Four

Conclusions

Chapter Overview

This chapter examines the case of a satellite main engine firing to perform a maneuver into a transfer orbit and how this affects the probability of detection. It also lists some of the best deployment times, presents the limitations of this study and recommendations for further study.

Maneuver Example

Since NORAD desires early indications of space events, the lack of radar coverage in the Southern Hemisphere presents a problem, should the satellite be deployed at a descending node. Eighty percent of the time that the shuttle arrives at a descending node, it may deploy a satellite with complete confidence it will not be observed until well after the satellite has reached the next node and ignited the main booster motor to perform a maneuver.

The inability to observe the last half of many orbits, in order to make an early determination of a satellite deployment, is rendered less important when the shuttle-satellite configuration passes over the next sensor. Even a sensor viewing the pair soon after a maneuver burn by the satellite to place it into a higher orbit will be able to distinquish the two objects. For example, say a class A naval reconnaissance satellite is deployed at the descending node of Rev 17 at a velocity of 5 meters / second along the shuttle's velocity vector. It is unobserved, and at the ascending node of Rev 18, the satellite main engine fires to boost the apogee of this transfer orbit to the 445 km operational altitude. Approximately six and a half minutes later, the radar at Antigua Island has the best opportunity to view the shuttle and satellite. The apparent angular separation could be as much as 9°, which could easily be detected by the radar. Even if the most pessimistic viewing geometry existed, so that the apparent angular separation angle was 0°, the apparent range difference would be nearly 360 km. The true range distance is almost 23 km, and even this is much more than the 750 meter range resolution of the Antigua radar, so the radar will be able to tell that there are two distinct objects in space.

In short, there is an overall high probability of detecting a satellite deployment from a Soviet shuttle.

Best Deployment Times

In looking through the ground trace maps in Appendix A, one may notice that there are several times in the first thirty orbits where the shuttle may go for almost an entire orbital period without being observed. From 60° true anomaly of Rev 6 to 40° true anomaly of Rev 7, the shuttle avoids all NORAD radars; this is a total of 340°, or 1.428 hours. This situation also occurs for Rev 12, 142° to Rev 13, 125° (total of 343°); Rev 13, 162° to Rev 14, 147° (total of 345°); Rev 26, 143° to Rev 27, 90° (total of 307°) and Rev 27, 146° to Rev 28, 138° (total of 352°). These opportunities exist for other deployment schemes that do not require initial separation at a node.

Limitations of this study

This analysis examined only the first two days (thirty revolutions) of a shuttle mission; a seven day mission is not unlikely, with satellite deployments possible to the last day. Only three directions for injection were examined; a particular satellite system might require a certain direction so that on-board sensors may be properly aligned to its target. The NORAD radar viewing angles were only briefly modeled, and a pessimistic viewing geometry of sensor, shuttle and satellite was assumed. The orbital mechanics model was the ideal, two-body case; no orbital perturbations were taken into account. Also, if the shuttle were allowed to maneuver, it could possibly avoid one or two radars, and greatly increase the time between being observed by the NORAD radars.

Recommendations for Further Analysis

The primary recommendation is to better model the location and viewing angles of the NORAD radars. The best course of action would be to use the actual data processing computer in NORAD's Cheyenne Mountain Complex; this would give realistic viewing angles (called "look angles" at the NCMC). The orbits of the shuttle and satellite could also be more closely modeled, so there could be a more realistic determination of range difference and angular separation.

Deployment direction needs further examination. Is there a more likely direction for satellite deployment than the three presented here?

The question of whether of not the U.S.S.R. can successfully hide a satellite deployment from the U.S. has not been fully answered; this thesis is only a first attempt at providing an answer; it appears to be "highly unlikely", but other schemes for deployment need to be thought of and examined. This preliminary answer also assumes that all the radars will be operating and tracking the shuttle the entire time it is within view. Since the U.S.S.R. has not yet launched a shuttle, no tasking procedures exist for tracking it. They need to be developed and tested to avoid the possiblilty that the shuttle could "slip through" if a site were not tracking it, deploy a satellite, and have it damage national security while the U.S. is ignorant of its presence.

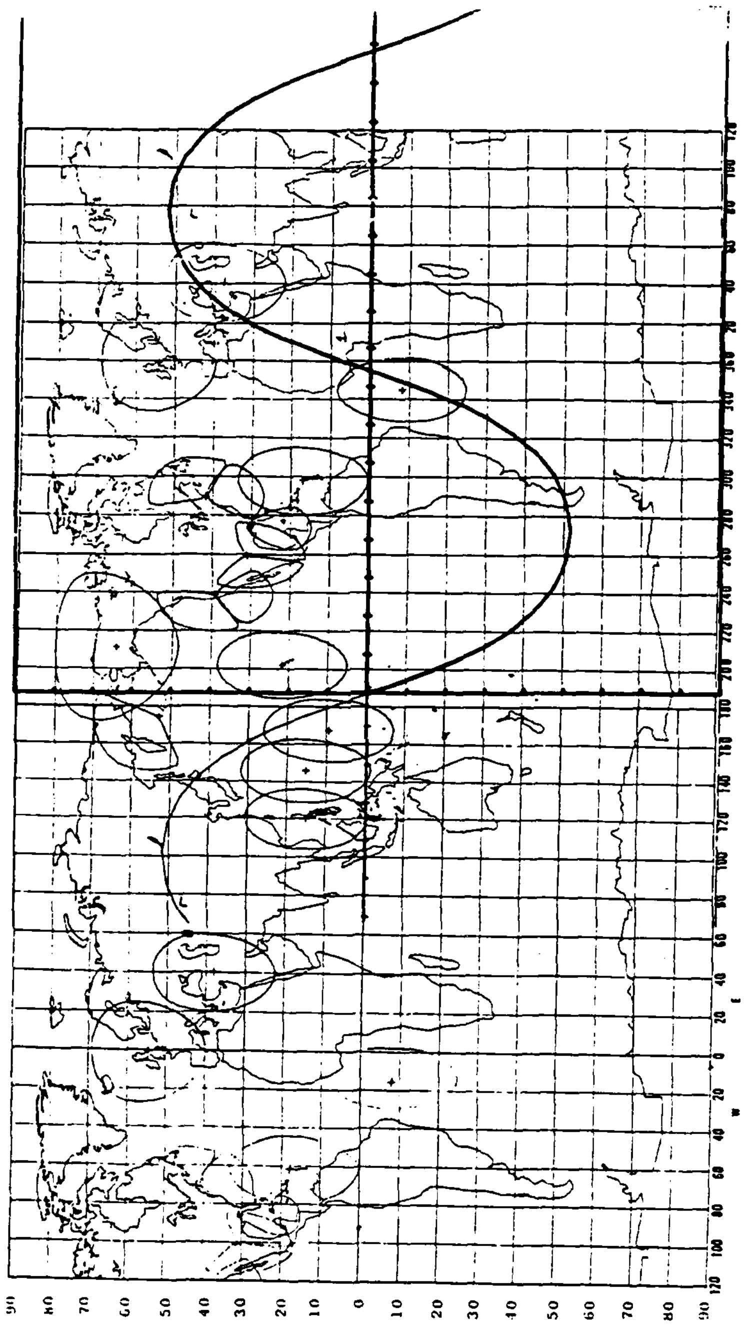

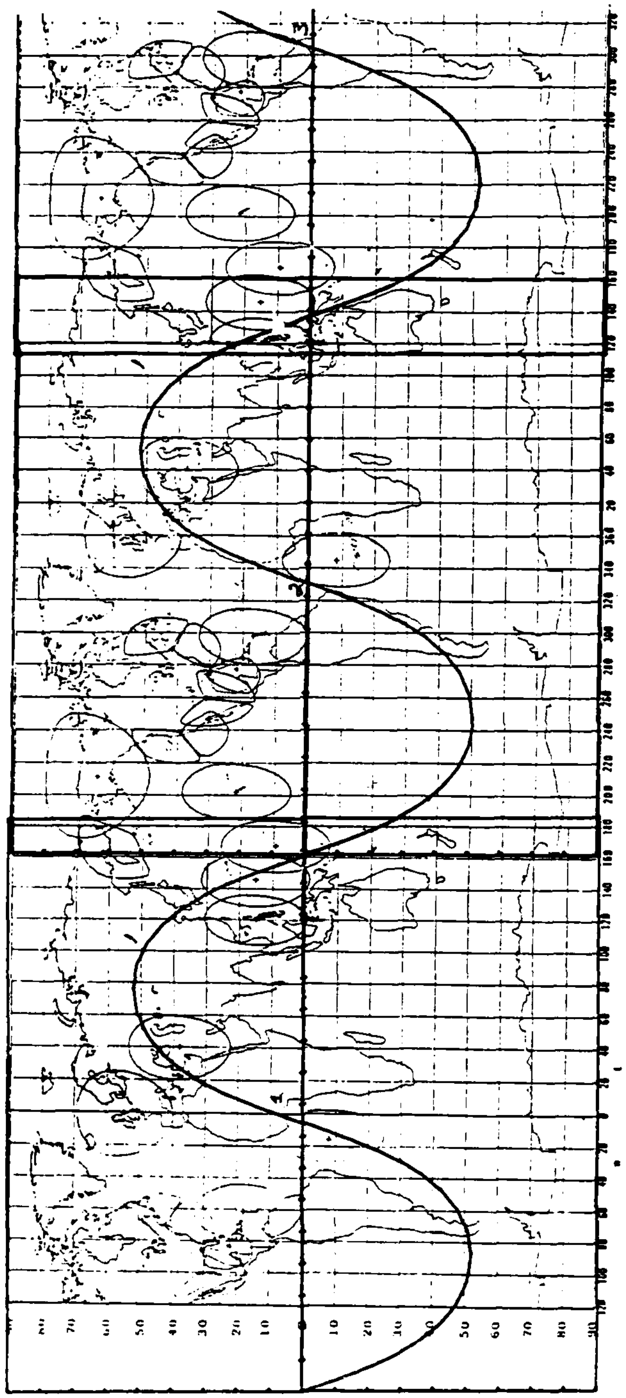

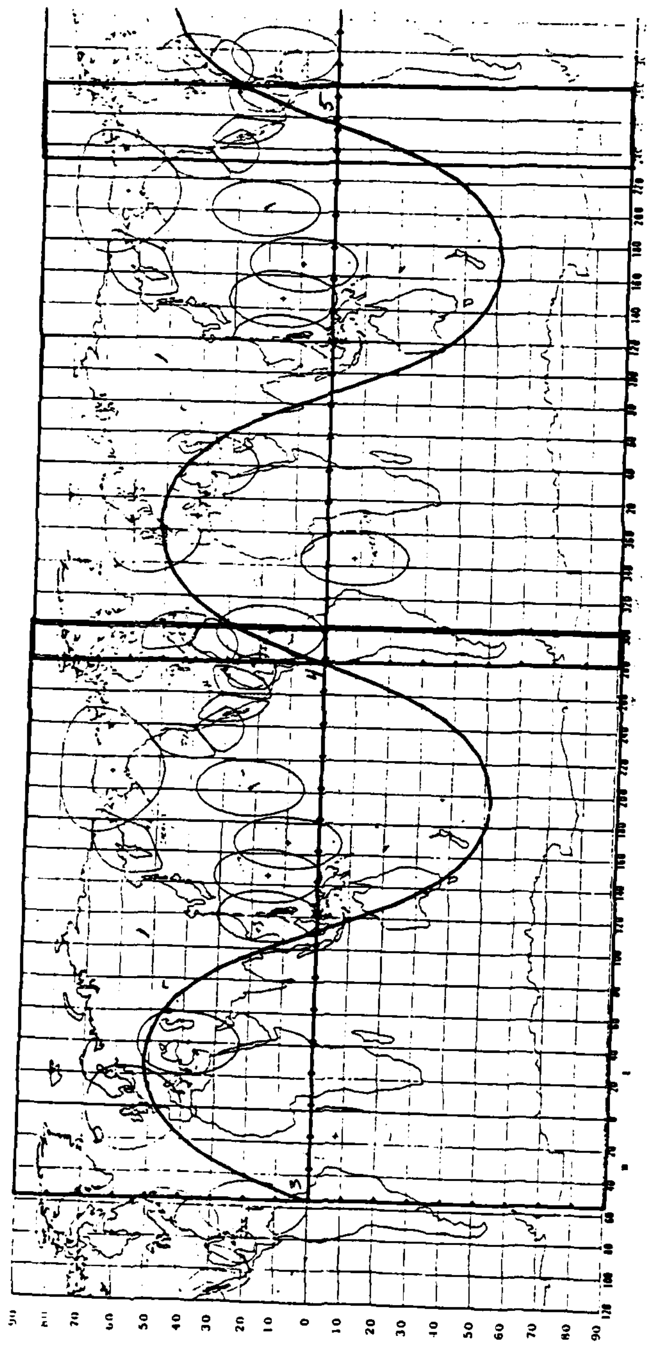

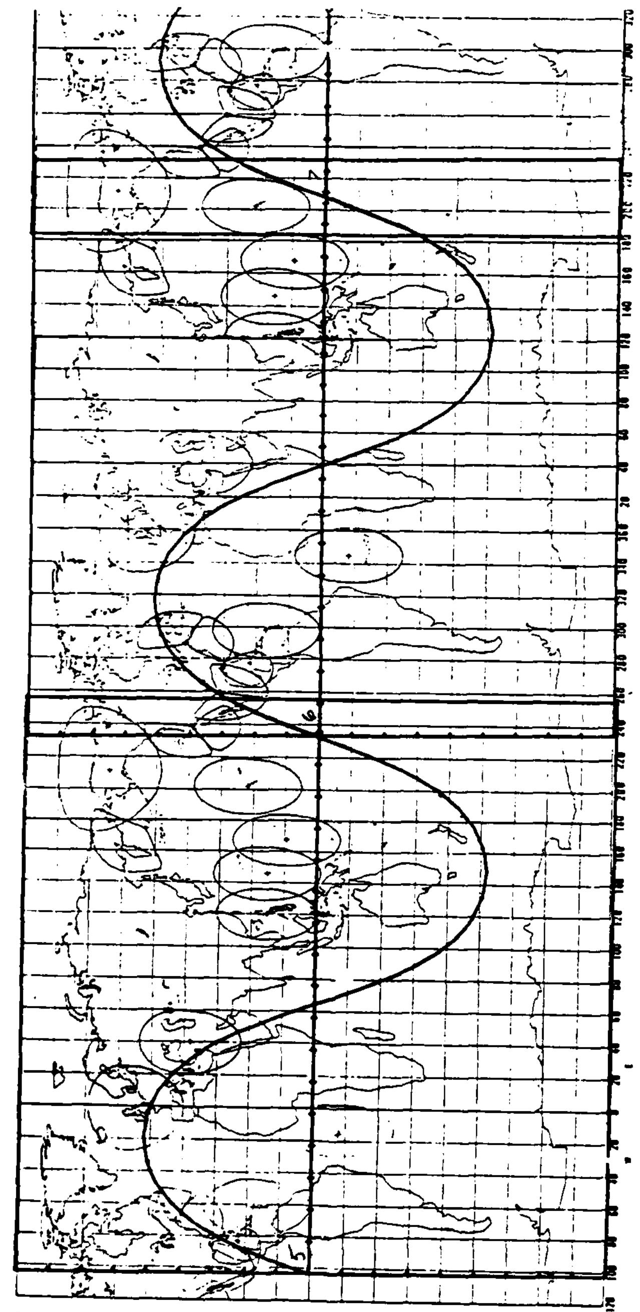

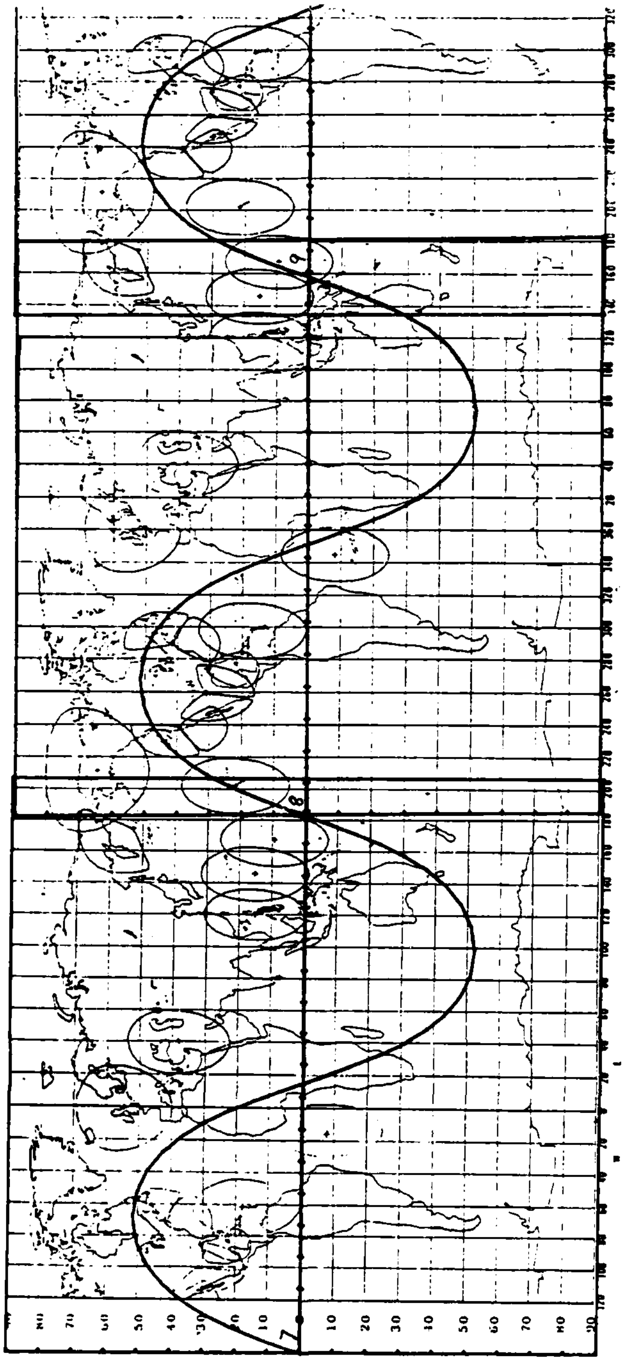

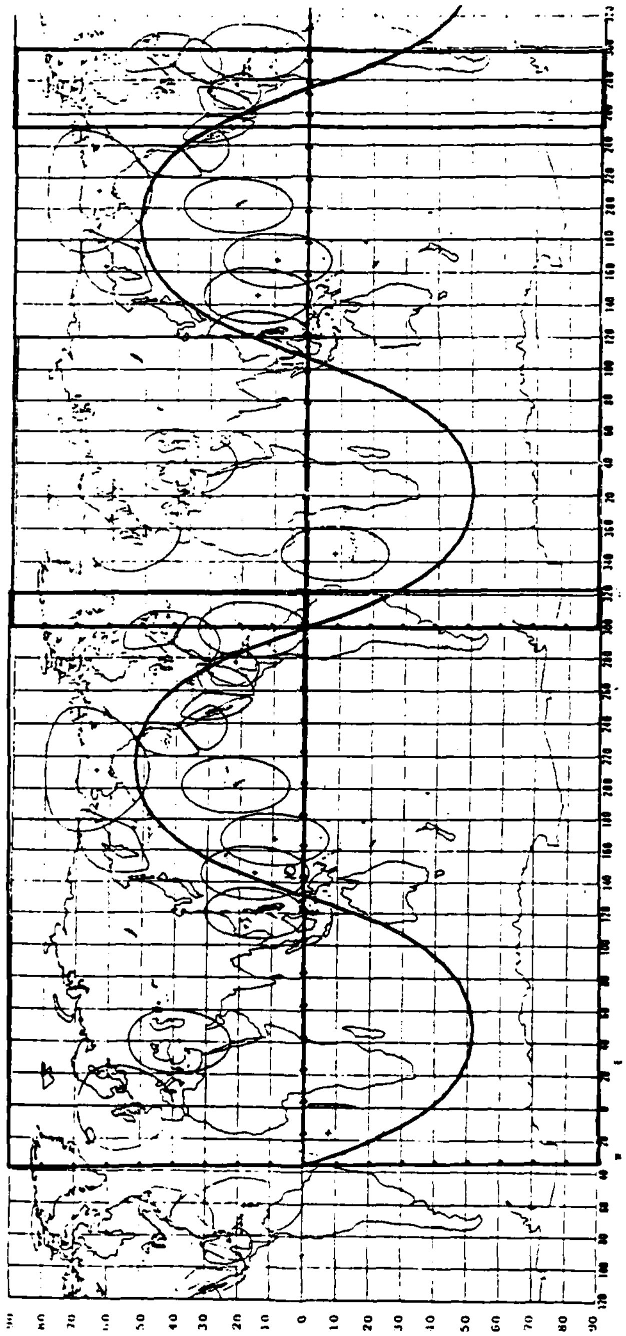

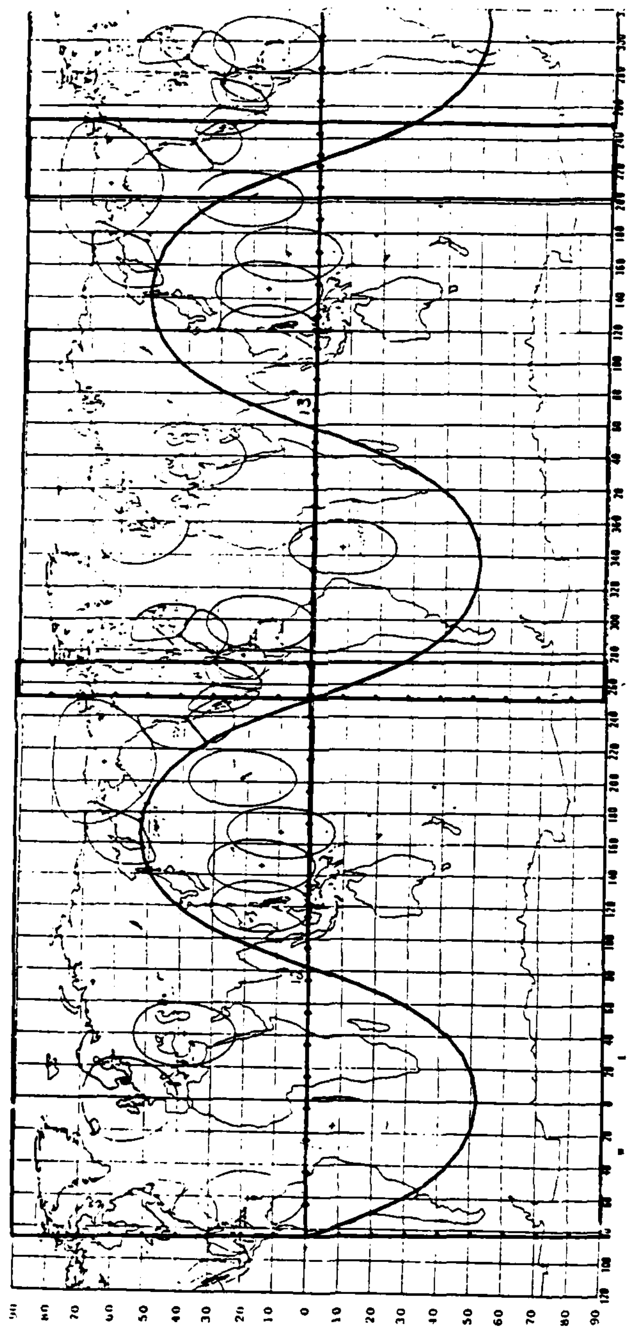

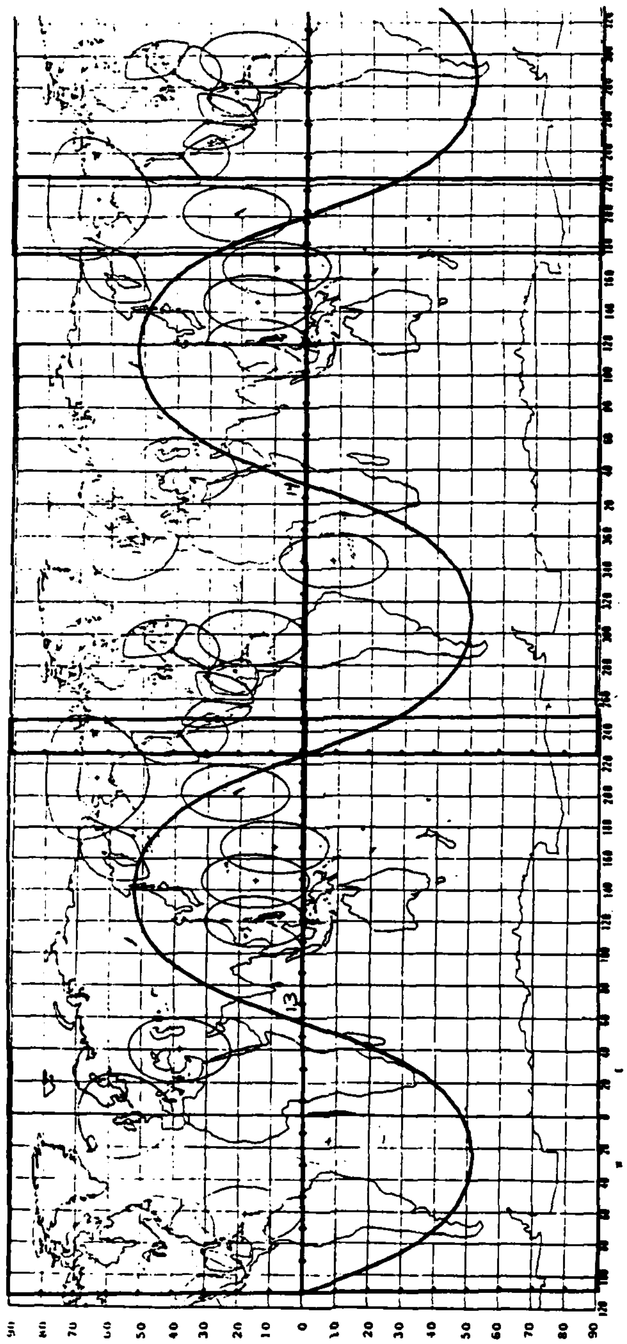

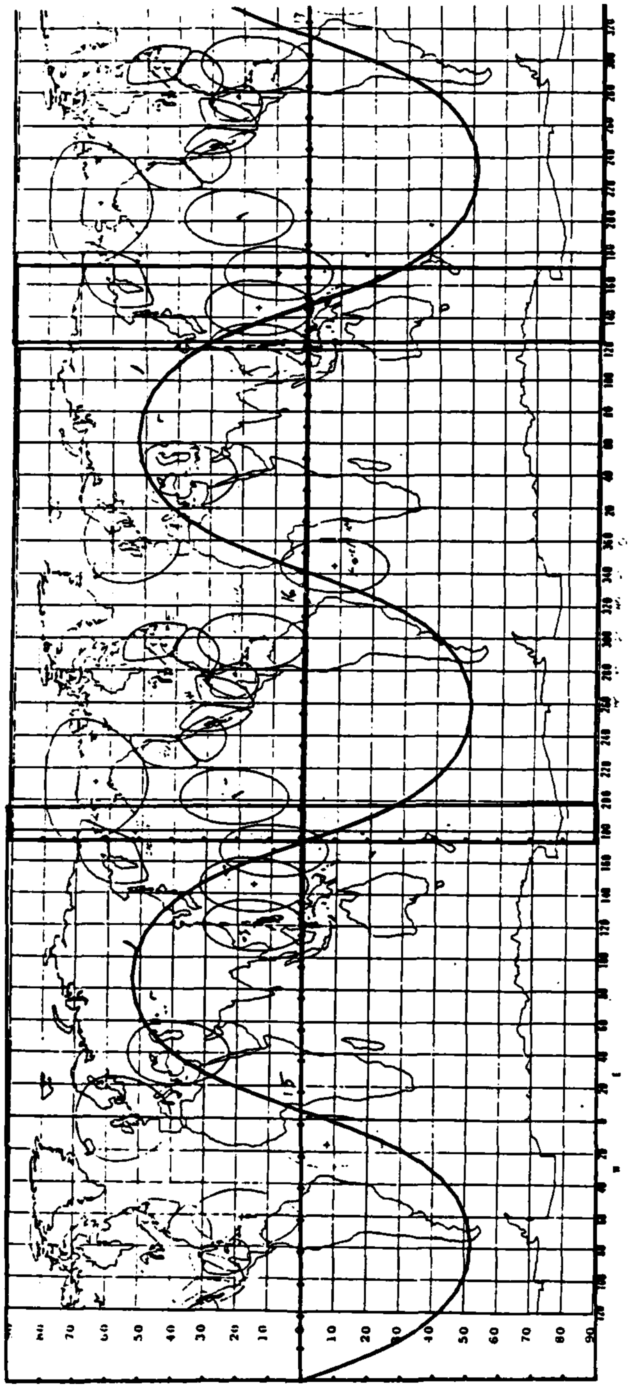

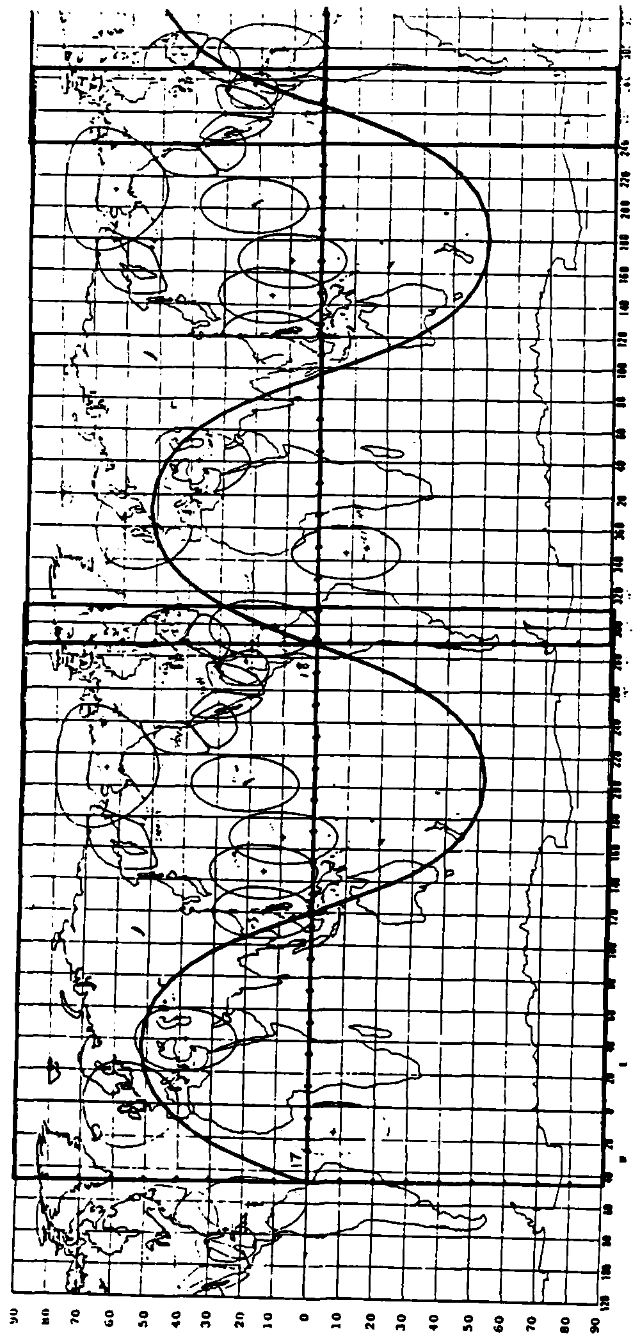

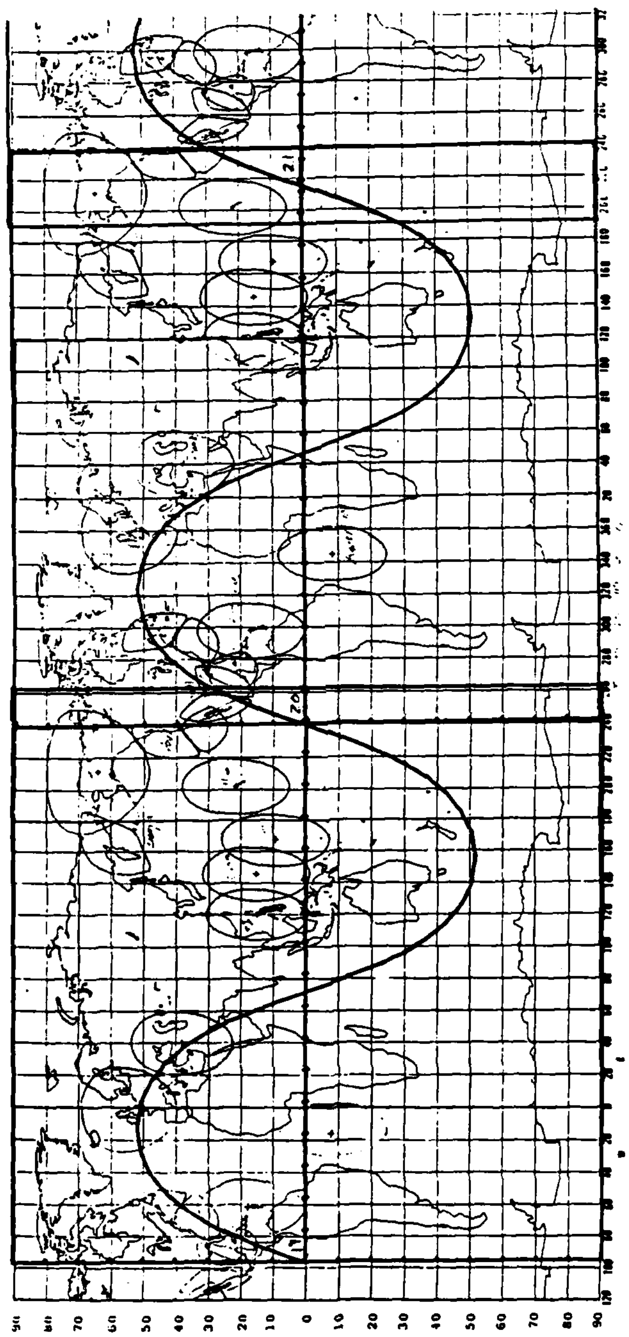

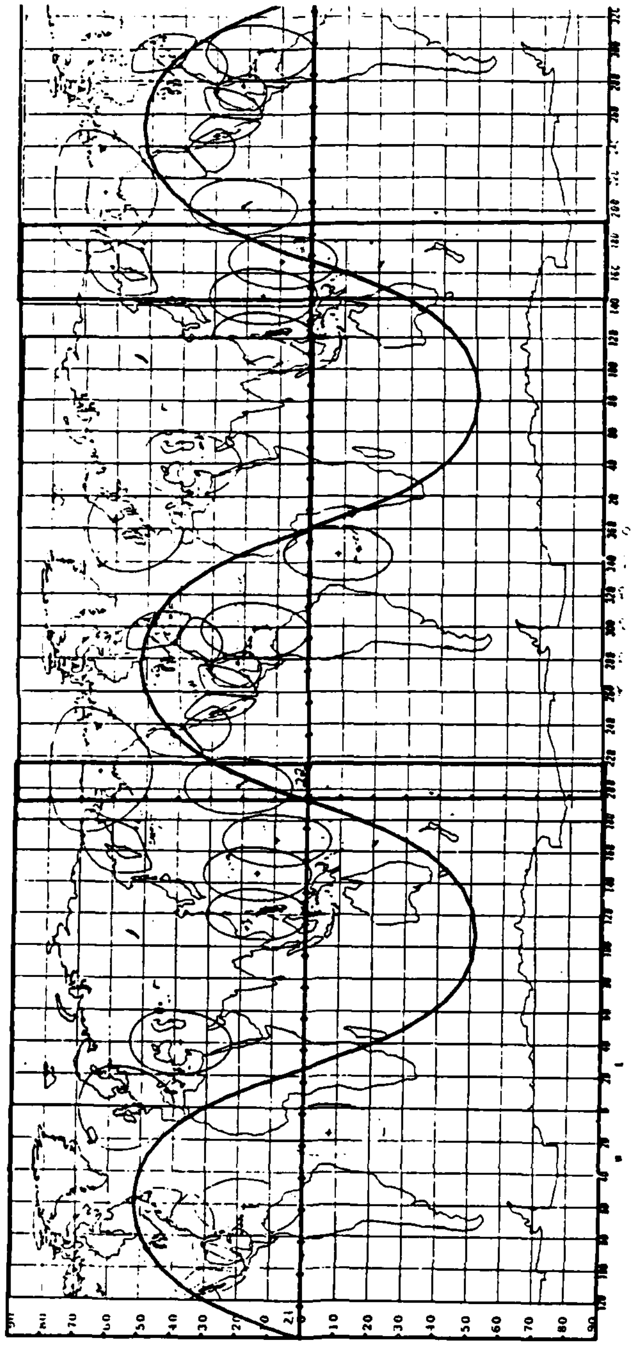

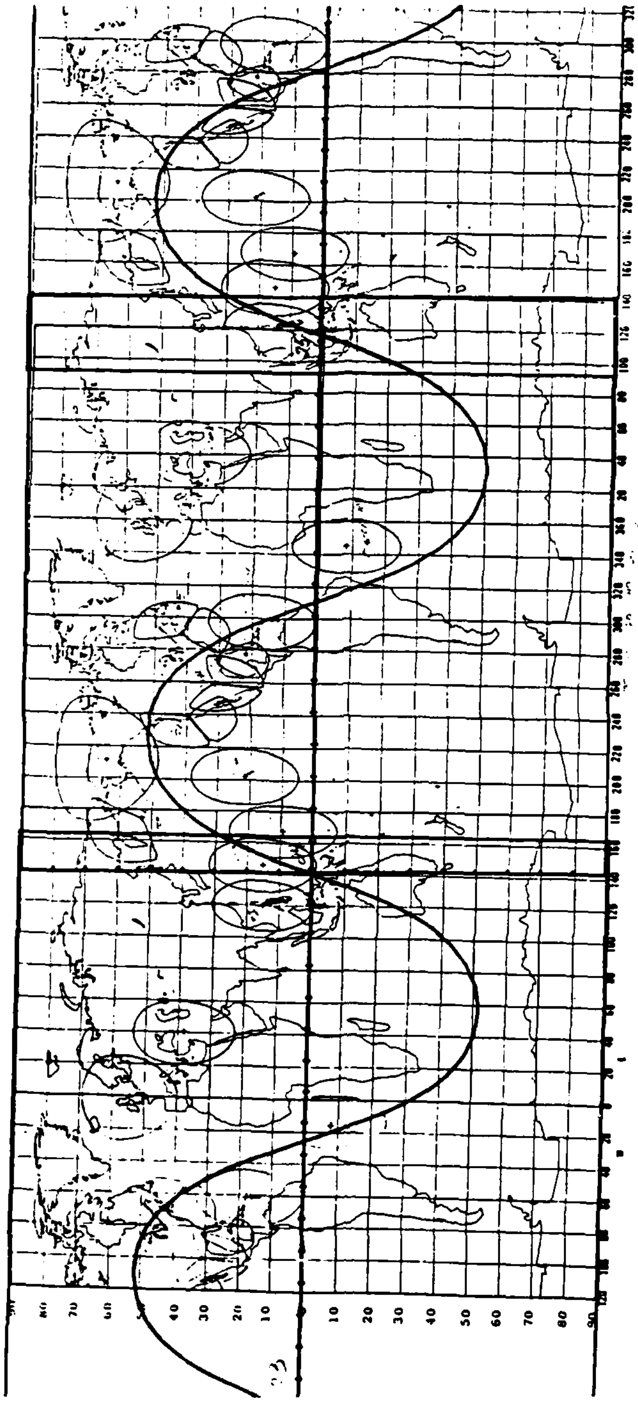

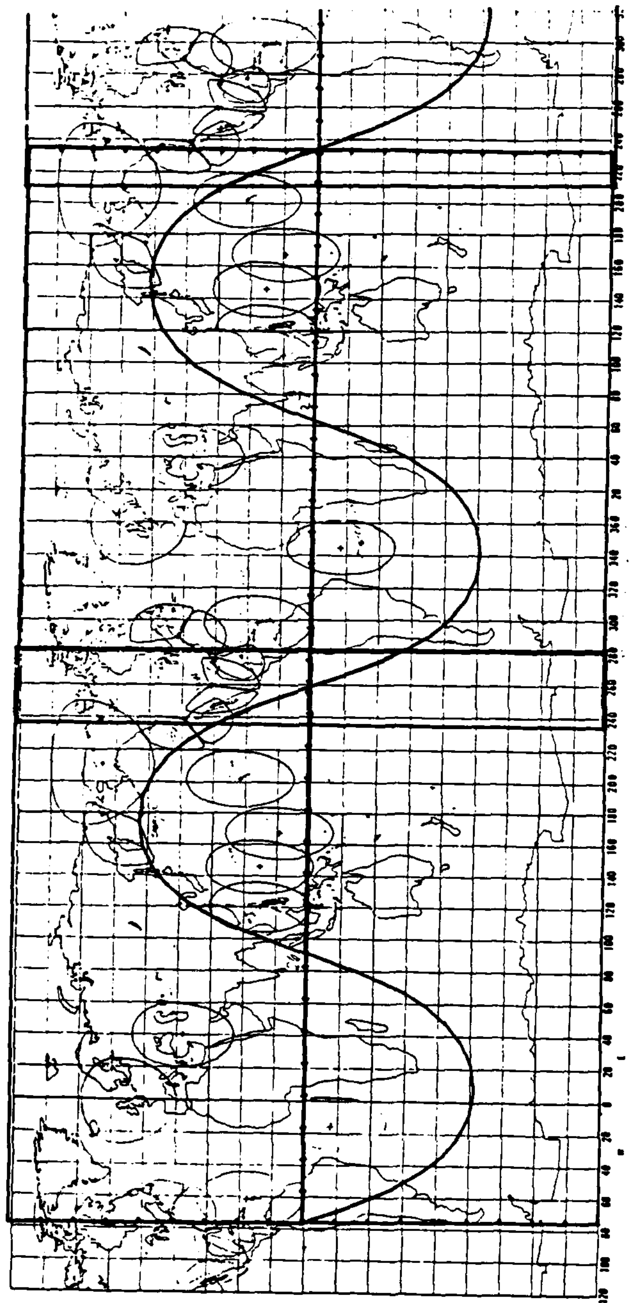

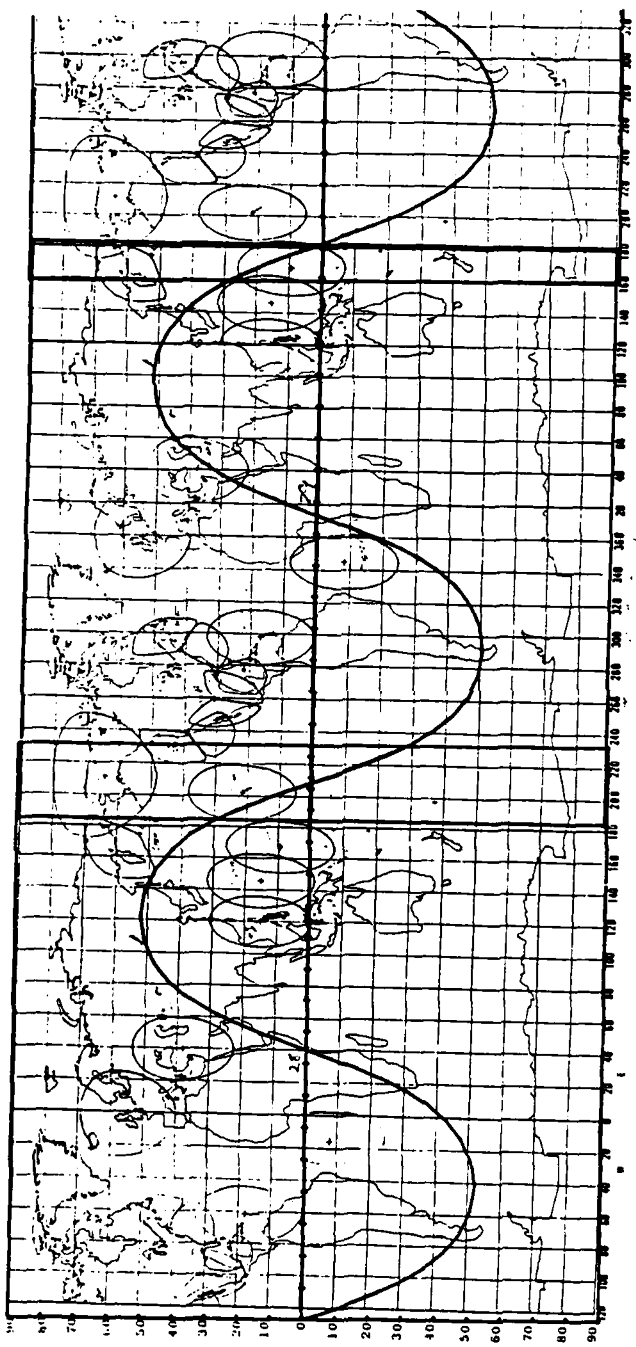

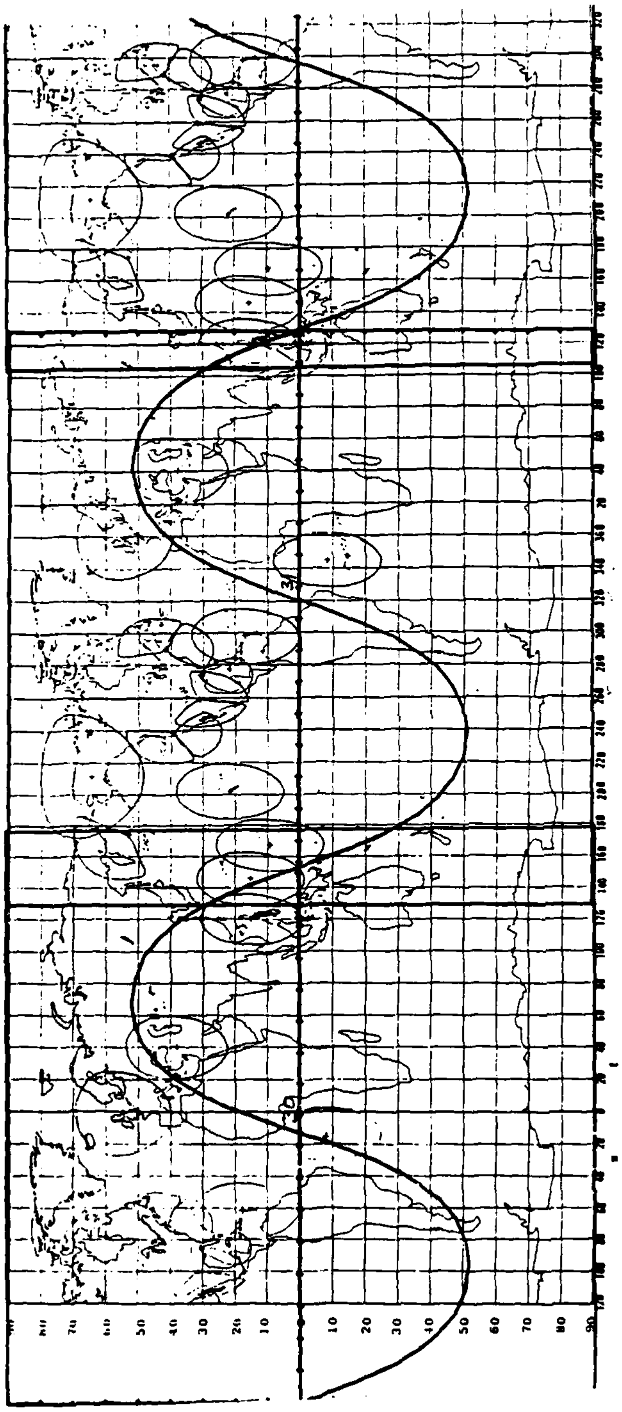

1. This program gives position and velocity vectors from a Keplerian element set

```
CLS
PRINT "This program gives r and v vectors from Keplerian element set."
DEFDBL A-Z
INPUT "semi-major axis (km) "; a
INPUT "eccentricity "; ecc
INPUT "inclination "; inc
INPUT "right ascension of ascending node "; omega
INPUT "argument of perigee "; argper
INPUT "true anomoly"; theta
INPUT "epoch time at ascending node (decimal hrs) "; timean
'*********** vectors *****************
theta = theta * .01745329252#  'radians
inc = inc * .01745329252#  'radians
omega = omega * .01745329252#  'radians
argper = argper * .01745329252#  'radians
p = a * (1 -ecc^2)
r = p / (1 + ecc * COS(theta))
rsubp = r * COS(theta)
rsubq = r * SIN(theta)
vsubp = -SIN(theta) * SQR(398601.2 / p)
vsubq = (ecc + COS(theta)) * SQR(398601.2 / p)
rsubx = ((COS(argper)*COS(omega)-SIN(argper)*SIN(omega) *COS(inc))
*rsubp) +  ((-SIN(argper)*COS(omega)-COS(argper)*SIN(omega)*COS(inc))
*rsubq)
rsuby = ((COS(argper)*SIN(omega)+SIN(argper)*COS(omega)*COS(inc))
*rsubp) + ((-SIN(argper)*SIN(omega)+COS(argper)*COS(omega)*COS(inc))
*rsubq)
rsubz = (SIN(argper)*SIN(inc)*rsubp) + (COS(argper)*SIN(inc)*rsubq)
vsubx = ((COS(argper)*COS(omega)-SIN(argper)*SIN(omega)*COS(inc))
*vsubp) + ((-SIN(argper)*COS(omega)-COS(argper)*SIN(omega)*COS(inc))
*vsubq)
vsuby = ((COS(argper)*SIN(omega)+SIN(argper)*COS(omega)*COS(inc))
*vsubp) + ((-SIN(argper)*SIN(omega)+COS(argper)*COS(omega)*COS(inc))
*vsubq)
vsubz = (SIN(argper)*SIN(inc)*vsubp) + (COS(argper)*SIN(inc)*vsubq)
r = SQR(rsubx^2 + rsuby^2 + rsubz^2)
v = SQR(vsubx^2 + vsuby^2 + vsubz^2)
ursubx = rsubx / r      'unit vectors
ursuby = rsuby / r
ursubz = rsubz / r
```

```
uvsubx = vsubx / v
uvsuby = vsuby / v
uvsubz = vsubz / v
Hsubx = (rsuby * vsubz) - (rsubz * vsuby)
Hsuby = (rsubz * vsubx) - (rsubx * vsubz)
Hsubz = (rsubx * vsuby) - (rsuby * vsubx)
H = SQR(Hsubx^2 + Hsuby^2 + Hsubz^2)
uHsubx = Hsubx / H
uHsuby = Hsuby / H
uHsubz = Hsubz / H
'************ times of flight ********************************
eccanom = 2 * ATN(SQR((1-ecc)/(1+ecc)) * TAN(theta/2))
eccargper = 2 * ATN(SQR((1-ecc)/(1+ecc)) * TAN(argper/2))
kat = SQR(a^3 / 398601.2) / 3600  'decimal hrs
tofanper = (eccargper - ecc * SIN(eccargper)) * kat  'time of flight from A.N.
to perigee
toffper = (eccanom - ecc * SIN(eccanom)) * kat  'time of flight from perigee
timeper = timean + tofanper
timev = timeper + toffper
period = 6.283185308# * kat
'************* output **************
theta = theta / .01745329252#  'degrees
inc = inc / .01745329252#  'degrees
omega = omega / .01745329252#  'degrees
argper = argper / .01745329252#  'degrees
LPRINT "semi-major axis (km) = "; a
LPRINT "eccentricity = "; ecc
LPRINT "inclination = "; inc
LPRINT "right ascension of ascending node = "; omega
LPRINT "argument of perigee = "; argper
LPRINT "true anomoly = "; theta
LPRINT "epoch time at ascending node (decimal hrs) = "; timean
LPRINT "time at perigee = "; timeper
LPRINT "time at vectors = "; timev
LPRINT "period (decimal hrs) = "; period
LPRINT "r (km) = "; r, "v (km/sec) = "; v
LPRINT "r sub x = "; rsubx
LPRINT "r sub y = "; rsuby
LPRINT "r sub z = "; rsubz
LPRINT "v sub x = "; vsubx
LPRINT "v sub y = "; vsuby
LPRINT "v sub z = "; vsubz
```

```
LPRINT "unit vector r sub x = "; ursubx
LPRINT "unit vector r sub y = "; ursuby
LPRINT "unit vector r sub z = "; ursubz
LPRINT "unit vector v sub x = "; uvsubx
LPRINT "unit vector v sub y = "; uvsuby
LPRINT "unit vector v sub z = "; uvsubz
LPRINT "H (km^2/sec) = "; H
LPRINT "H sub x = "; Hsubx
LPRINT "H sub y = "; Hsuby
LPRINT "H sub z = "; Hsubz
LPRINT "unit vector H sub x = "; uHsubx
LPRINT "unit vector H sub y = "; uHsuby
LPRINT "unit vector H sub z = "; uHsubz
END
```

2. This program gives the Keplerian element set from the position and velocity vectors.

```
CLS
PRINT "This program gives the Keplerian elset from r and v vectors."
DEFDBL A-Z
DEF FNARCCOS(X) = -ATN(X / SQR(1 - X^2)) + 1.570796327#
INPUT "r sub i ="; rsubi
INPUT "r sub j ="; rsubj
INPUT "r sub k ="; rsubk
INPUT "v sub i ="; vsubi
INPUT "v sub j ="; vsubj
INPUT "v sub k ="; vsubk
INPUT "time at vectors (decimal hrs) ="; timev
r = SQR(rsubi^2 + rsubj^2 + rsubk^2)
v = SQR(vsubi^2 +vsubj^2 + vsubk^2)
'******* angular momentum vector h ********
hsubi = rsubj*vsubk - rsubk*vsubj
hsubj = rsubk*vsubi - rsubi*vsubk
hsubk = rsubi*vsubj - rsubj*vsubi
h = SQR(hsubi^2 + hsubj^2 + hsubk^2)
'******* node vector n ***********
nsubi = -hsubj
nsubj = hsubi
nsubk = 0
n = SQR(nsubi^2 + nsubj^2)
```

```
'******* eccentricity vector ecc *********
factorone = (v^2 / 398601.2) - (1/r)
factortwo = (rsubi*vsubi + rsubj*vsubj + rsubk*vsubk) / 398601.2
esubi = factorone * rsubi - factortwo * vsubi
esubj = factorone * rsubj - factortwo * vsubj
esubk = factorone * rsubk - factortwo * vsubk
ecc = SQR(esubi^2 + esubj^2 + esubk^2)
'***** semi-major axis ********
p = h^2 / 398601.2
a = p / (1 -ecc^2)
'****** inclination ********
cosinc = hsubk / h
inc = FNARCCOS(cosinc) / .01745329252#  'division gives inc in degrees
'****** right ascension of the ascending node **********
cosomega = nsubi / n
IF cosomega < = -1 THEN omega = 180
IF cosomega < = -1 THEN GOTO workarnd1
omega = FNARCCOS(cosomega) / .01745329252#   'degrees
IF nsubj < 0 THEN omega = 360 - omega
workarnd1: '******** argument of perigee *********
cosargper = (nsubi*esubi + nsubj*esubj + nsubk*esubk) / (n*ecc)
argper = FNARCCOS(cosargper)
IF esubk < 0 THEN argper = 6.283185308# - argper
'******* true anomoly *****************
costheta = (esubi * rsubi + esubj * rsubj + esubk * rsubk) / (ecc * r)
theta = FNARCCOS(costheta)
IF factortwo < 0 THEN theta = 6.283185308# - theta
'*********** Times of flight **********
eccanom = 2 * ATN(SQR((1 - ecc) / (1 + ecc)) * TAN(theta / 2))
eccargper = 2 * ATN(SQR((1 - ecc) /(1 + ecc)) * TAN(argper / 2))
kat = SQR(a^3 / 398601.2) / 3600  'decimal hrs
tofanper = (eccargper - ecc * SIN(eccargper)) * kat  'time of flight from A.N.
to perigee
toffper = (eccanom - ecc * SIN(eccanom)) * kat  'time of flight from perigee
timeper = timev - toffper  'time at perigee
timean = timeper - tofanper  'time at ascending node
period = 6.283185308# * kat
argper = argper / .01745329252#  'degrees
theta = theta / .01745329252#  'degrees
'************* OUTPUT ************
LPRINT "r sub i ="; rsubi
LPRINT "r sub j ="; rsubj
LPRINT "r sub k ="; rsubk
```

```
LPRINT "v sub i ="; vsubi
LPRINT "v sub j ="; vsubj
LPRINT "v sub k ="; vsubk
LPRINT "time at vectors (decimal hrs) ="; timev
LPRINT "semi-major axis (km) = "; a
LPRINT "eccentricity = "; ecc
LPRINT "inclination = "; inc
LPRINT "argument of perigee = "; argper
LPRINT "right ascension of ascending node = "; omega
LPRINT "true anomoly = "; theta
LPRINT "time at perigee (decimal hrs) = "; timeper
LPRINT "time at ascending node (decimal hrs) = "; timean
LPRINT "period (decimal hrs) = "; period
END
```

3. This program gives the right ascension and delination position from the Keplerian element set.

```
CLS
PRINT "This program gives right ascension and declination from Keplerian
elset."
DEFDBL a-z : DIM eccanom(50), f(50), fprime(50)
DEF FNarcsin(x) = ATN(x / SQR(1 - x^2))
INPUT "Epoch time at ascending node (decimal hrs) ="; timean
INPUT "Elapsed time from epoch (decimal hrs) ="; telapse
INPUT "semi-major axis (km) ="; a
INPUT "eccentricity ="; ecc
INPUT "argument of perigee (in degrees) ="; argper
INPUT "right ascension of ascending node ="; omega
INPUT "inclination ="; inc
argper = argper * .01745329252#  'radians
omega = omega * .01745329252#  'radians
inc = inc * .01745329252#  'radians
REM *******Kepler problem**********
kat = SQR(a^3 / 398601.2) / 3600  'decimal hrs
eccargper = 2 * ATN(SQR((1 - ecc) / (1 + ecc)) * TAN(argper / 2))
tofanper = (eccargper - ecc * SIN(eccargper)) * kat  'time of flight from A.N.
to perigee
toffper = telapse - tofanper
period = 6.283185308# * kat
REM *******Newton-Raphson iteration**********
n = 0 : eccanom(0) = toffper / kat  ' first guess, equal to Mean anomoly
```

```
Newton:
   f(n) = eccanom(n) - ecc * SIN(eccanom(n)) - eccanom(0)
   fprime(n) = 1 - ecc * COS(eccanom(n))
   eccanom(n+1) = eccanom(n) - ( f(n) / fprime(n) )
   IF eccanom(n+1) = eccanom(n) THEN GOTO Polar
   n = n + 1: GOTO Newton
Polar: '*******Perifocal coordinates***********
theta = 2 * ATN(SQR((1 + ecc) / (1 - ecc)) * TAN (eccanom(n) / 2))
r = (a * (1 - ecc^2)) / (1 + ecc * COS(theta))
xw = r * COS(theta) : yw = r * SIN(theta) : zw = 0
theta = theta / .01745329252#  'degrees
Inertial: '*********Inertial coordinates*********
xe = ((COS(argper)*COS(omega)-SIN(argper)*SIN(omega)*COS(inc))*xw)
+ ((-SIN(argper)*COS(omega)-COS(argper)*SIN(omega)*COS(inc))*yw)
ye = ((COS(argper)*SIN(omega)+SIN(argper)*COS(omega)*COS(inc))*xw)
+ ((-SIN(argper)*SIN(omega)+COS(argper)*COS(omega)*COS(inc))*yw)
ze = (SIN(argper)*SIN(inc)*xw) + (COS(argper)*SIN(inc)*yw)
alpha = (ATN(ye / xe)) / .01745329252#  'degrees
IF alpha < 0 THEN alpha = alpha + 360
dec = (FNarcsin(ze / r)) / .01745329252#  'degrees
codec = 90 - dec
timeper = timean + tofanper
argper = argper / .01745329252#  'degrees
omega = omega / .01745329252#  'degrees
inc = inc / .01745329252#  'degrees
LPRINT "Keplerian elset"
LPRINT "Epoch time at ascending node (decimal hrs) ="; timean
LPRINT "Elapsed time from epoch (decimal hrs) ="; telapse
LPRINT "Epoch time at perigee (decimal hrs) = "; timeper
LPRINT "period (decimal hrs) = "; period
LPRINT "semi-major axis (km) ="; a
LPRINT "eccentricity ="; ecc
LPRINT "argument of perigee (in degrees) ="; argper
LPRINT "right ascension of ascending node ="; omega
LPRINT "inclination ="; inc
LPRINT "radius (km) = "; r
LPRINT "r sub x = "; xe
LPRINT "r sub y = "; ye
LPRINT "r sub z = "; ze
LPRINT "true anomoly = "; theta
LPRINT "right ascension ="; alpha
LPRINT "declination ="; dec
LPRINT "co-declination ="; codec
END
```

4. This program gives right ascension and declination values, range and angular separation distances from position and velocity vectors.

```
CLS
PRINT "This program gives RA and dec from vectors"
DEFDBL a-z : DIM eccanom(50), f(50), fprime(50)
DEF FNARCCOS(X) = -ATN(X / SQR(1 - X^2)) + 1.570796327#
DEF FNarcsin(x) = ATN(x / SQR(1 - x^2))
PRINT "Is deployment vector along the r vector ? Enter '1' "
PRINT "or is it along the v vector ? Enter '2' "
PRINT "or is it along the H vector ? Enter '3' "
INPUT choice
IF choice = 1 THEN LPRINT "Deployment along r vector"
IF choice = 2 THEN LPRINT "Deployment along v vector"
IF choice = 3 THEN LPRINT "Deployment along H vector"
PRINT "The following 8 values are for the satellite"
INPUT "Epoch time at ascending node (decimal hrs) ="; timean
INPUT "r sub i ="; rsubi
INPUT "r sub j ="; rsubj
INPUT "r sub k ="; rsubk
INPUT "v sub i ="; vsubi
INPUT "v sub j ="; vsubj
INPUT "v sub k ="; vsubk
INPUT "time at vectors (decimal hrs) ="; timev
PRINT
Comeagain: INPUT "true anomaly at sensor for shuttle = "; seen
INPUT "elevation of shutle = "; el
INPUT "slant range of shuttle = "; SL
el = el * .01745329252#   'radians
LPRINT : LPRINT "True anomaly at sensor for shuttle = "; seen
telapse = seen * .004200143#
r = SQR(rsubi^2 + rsubj^2 + rsubk^2)
v = SQR(vsubi^2 +vsubj^2 + vsubk^2)
'******* angular momentum vector h ********
hsubi = rsubj*vsubk - rsubk*vsubj
hsubj = rsubk*vsubi - rsubi*vsubk
hsubk = rsubi*vsubj - rsubj*vsubi
h = SQR(hsubi^2 + hsubj^2 + hsubk^2)
'******* node vector n ***********
nsubi = -hsubj
nsubj = hsubi
nsubk = 0
n = SQR(nsubi^2 + nsubj^2)
```

```
'******* eccentricity vector ecc *********
factorone = (v^2 / 398601.2) - (1/r)
factortwo = (rsubi*vsubi + rsubj*vsubj + rsubk*vsubk) / 398601.2
esubi = factorone * rsubi - factortwo * vsubi
esubj = factorone * rsubj - factortwo * vsubj
esubk = factorone * rsubk - factortwo * vsubk
ecc = SQR(esubi^2 + esubj^2 + esubk^2)
'***** semi-major axis ********
p = h^2 / 398601.2
a = p / (1 -ecc^2)
'****** inclination ********
cosinc = hsubk / h
inc = FNARCCOS(cosinc) / .01745329252#  'division gives inc in degrees
'****** right ascension of the ascending node **********
cosomega = nsubi / n
IF cosomega < = -1 THEN omega = 180
IF cosomega < = -1 THEN GOTO workarnd1
omega = FNARCCOS(cosomega) / .01745329252#   'degrees
IF nsubj < 0 THEN omega = 360 - omega
workarnd1: '******** argument of perigee *********
cosargper = (nsubi*esubi + nsubj*esubj + nsubk*esubk) / (n*ecc)
argper = FNARCCOS(cosargper)
IF esubk < 0 THEN argper = 6.283185308# - argper
'******* true anomoly *****************
costheta = (esubi * rsubi + esubj * rsubj + esubk * rsubk) / (ecc * r)
theta = FNARCCOS(costheta)
IF factortwo < 0 THEN theta = 6.283185308# - theta
'*********** Times of flight **********
eccanom = 2 * ATN(SQR((1 - ecc) / (1 + ecc)) * TAN(theta / 2))
eccargper = 2 * ATN(SQR((1 - ecc) /(1 + ecc)) * TAN(argper / 2))
kat = SQR(a^3 / 398601.2) / 3600  'decimal hrs
tofanper = (eccargper - ecc * SIN(eccargper)) * kat  'time of flight from A.N.
to perigee
toffper = (eccanom - ecc * SIN(eccanom)) * kat  'time of flight from perigee
timeper = timev - toffper  'time at perigee
timean = timeper - tofanper  'time at ascending node
period = 6.283185308# * kat
argper = argper / .01745329252#  'degrees
theta = theta / .01745329252#  'degrees
'************* OUTPUT ************
' LPRINT "r sub i ="; rsubi
' LPRINT "r sub j ="; rsubj
' LPRINT "r sub k ="; rsubk
```

```
' LPRINT "v sub i ="; vsubi
' LPRINT "v sub j ="; vsubj
' LPRINT "v sub k ="; vsubk
' LPRINT "time at vectors (decimal hrs) ="; timev
' LPRINT "semi-major axis (km) = "; a
' LPRINT "eccentricity = "; ecc
' LPRINT "inclination = "; inc
' LPRINT "argument of perigee = "; argper
' LPRINT "right ascension of ascending node = "; omega
' LPRINT "true anomoly = "; theta
' LPRINT "time at perigee (decimal hrs) = "; timeper
' LPRINT "time at ascending node (decimal hrs) = "; timean
' LPRINT "period (decimal hrs) = "; period
argper = argper * .01745329252#  'radians
omega = omega * .01745329252#  'radians
inc = inc * .01745329252#  'radians
REM *******Kepler problem**********
kat = SQR(a^3 / 398601.2) / 3600  'decimal hrs
eccargper = 2 * ATN(SQR((1 - ecc) / (1 + ecc)) * TAN(argper / 2))
tofanper = (eccargper - ecc * SIN(eccargper)) * kat  'time of flight from A.N.
to perigee
toffper = telapse - tofanper
period = 6.283185308# * kat
REM *******Newton-Raphson iteration**********
n = 0 : eccanom(0) = toffper / kat  ' first guess, equal to Mean anomoly
Newton:
   f(n) = eccanom(n) - ecc * SIN(eccanom(n)) - eccanom(0)
   fprime(n) = 1 - ecc * COS(eccanom(n))
   eccanom(n+1) = eccanom(n) - ( f(n) / fprime(n) )
   IF eccanom(n+1) = eccanom(n) THEN GOTO Polar
   n = n + 1: GOTO Newton
Polar: '*******Perifocal coordinates***********
theta = 2 * ATN(SQR((1 + ecc) / (1 - ecc)) * TAN (eccanom(n) / 2))
r = (a * (1 - ecc^2)) / (1 + ecc * COS(theta))
xw = r * COS(theta) : yw = r * SIN(theta) : zw = 0
theta = theta / .01745329252#  'degrees
Inertial: '*********Inertial coordinates*********
xe = ((COS(argper)*COS(omega)-SIN(argper)*SIN(omega)*COS(inc))*xw)
+ ((-SIN(argper)*COS(omega)-COS(argper)*SIN(omega)*COS(inc))*yw)
ye = ((COS(argper)*SIN(omega)+SIN(argper)*COS(omega)*COS(inc))*xw)
+ ((-SIN(argper)*SIN(omega)+COS(argper)*COS(omega)*COS(inc))*yw)
ze = (SIN(argper)*SIN(inc)*xw) + (COS(argper)*SIN(inc)*yw)
alpha = ATN(ye / xe)
```

```
IF xe < 0 THEN alpha = alpha + 3.141592654#
IF ye < 0 AND xe > 0 THEN alpha = alpha + 6.283185308#
dec = FNarcsin(ze / r)
timeper = timean + tofanper
argper = argper / .01745329252#  'degrees
omega = omega / .01745329252#  'degrees
inc = inc / .01745329252#  'degrees
'********** shuttle section ************
seen = seen * .01745329252#
xwsh = 6688.145 * COS(seen)
ywsh = 6688.145 * SIN(seen)
xesh = -xwsh
yesh = (-.620874182#) * ywsh
zesh = .783910231# * ywsh
alphash = ATN(yesh / xesh)
IF xesh < 0 THEN alphash = alphash + 3.141592654#
IF yesh < 0 AND xesh > 0 THEN alphash = alphash + 6.283185308#
decsh = FNarcsin(zesh / 6688.145)
'*********** final outcome *************
interrange = ABS(r - 6688.145)
distance = SQR((xe - xesh)^2 + (ye - yesh)^2 + (ze - zesh)^2)
ang = FNarccos(SIN(dec) * SIN(decsh) + COS(dec) * COS(decsh) * COS(alpha -
alphash))
halfd = 6688.145 * SIN(ang / 2)
beta = 2 * FNarcsin(halfd / SL)
d = halfd * 2
h = SL * SIN(el)
j = (SL * COS(el)) - d
IF j < 0 THEN j = 0
comp = ATN(j / h)
k = SQR(SL^2 + d^2 - 2 * SL * d * COS(el))
phi = (FNarccos((SL^2 + k^2 - d^2) / (2 * SL * k))) / .01745329252#
ang = ang / .01745329252#
LPRINT "True range difference = "; interrange
LPRINT "True separation distance = "; distance
LPRINT "True angular separation = "; ABS(ang)
LPRINT "Fig 3 range difference = "; ABS(SL - k)
LPRINT "Fig 3 apparent angular separation = "; ABS(phi)
j = SL * SIN(el)
h = SL * COS(el)
IF h < 0 THEN h = 0
phi = ATN((interrange + j) / h) - el
IF phi < 0 THEN phi = 0
```

```
k = (interrange + j) / SIN(phi + el)
phi = phi / .01745329252#
LPRINT "Fig 5 range difference = "; ABS(SL - k)
LPRINT "Fig 5 apparent angular separation = "; ABS(phi)
' LPRINT "Keplerian elset"
' LPRINT "Epoch time at ascending node (decimal hrs) ="; timean
' LPRINT "Elapsed time from epoch (decimal hrs) ="; telapse
' LPRINT "Epoch time at perigee (decimal hrs) = "; timeper
' LPRINT "period (decimal hrs) = "; period
' LPRINT "semi-major axis (km) ="; a
' LPRINT "eccentricity ="; ecc
' LPRINT "argument of perigee (in degrees) ="; argper
' LPRINT "right ascension of ascending node ="; omega
' LPRINT "inclination ="; inc
' LPRINT "radius of satellite (km) = "; r
' LPRINT "r sub x (of satellite) = "; xe
' LPRINT "r sub y (of satellite) = "; ye
' LPRINT "r sub z (of satellite)= "; ze
' LPRINT "true anomoly (of satellite) = "; theta
' LPRINT "right ascension (of satellite) ="; alpha
' LPRINT "declination (of satellite) ="; dec
' LPRINT "shuttle xe = "; xesh
' LPRINT "shuttle ye = "; yesh
' LPRINT "shuttle ze = "; zesh
' LPRINT "shuttle RA = "; alphash
' LPRINT "shuttle dec = "; decsh
PRINT
GOTO Comeagain
Finis: END
```

BIBLIOGRAPHY

1. The Astronomical Almanac for the Year 1985. Washington, D.C.: U.S. Government Printing Office.

2. Baker, Robert M. L. and Maud W. Makemson. An Introduction to Astrodynamics. New York: Academic Press, 1967.

3. Baker, Robert M. L. Astrodynamics - Applications and Advanced Topics. New York: Academic Press, 1967.

4. Bate, Roger E., Donald D. Miller and Jerry E. White. Fundamentals of Astrodynamics. New York: Dover Publications, Inc., 1971.

5. Boyarski, USAF Capt David. Telephone interview, NORAD Cheyenne Mountain Complex, Colorado Springs, CO, 5 and 6 September 1985.

6. Bray, USAF Major James. HQ Space Command/DOSS. Telephone interview, HQ SPACECMD, Colorado Springs, CO, 5 and 13 August 1985.

7. Bray, USAF Major James. *HQ Space Command/DOSS*. Personal correspondance, HQ SPACECMD, Colorado Springs, CO, 28 August 1985.

8. Covault, Craig. "USSR's Reusable Orbiter Nears Approach, Landing Tests." Aviation Week and Space Technology, 121: 18-19 (Dec 3, 1984).

9. -----. "Soviets Building Heavy Shuttle." Aviation Week and Space Technology, 118: 255-259 (Mar 14, 1983).

10. -----. "Soviets Orbit Shuttle Vehicle." Aviation Week and Space Technology, 116: 18-19 (Jun 14, 1982).

11. Eagan, USAF Lt. Col. Director, HQ Space Command/DOSV. Telephone interview, HQ SPACECMD, Colorado Springs, CO, 25 July 1985.

12. Freedman, Jerome. "Resolution in Radar Systems." Radars, Vol 4, Radar Resolution and Multi-path Effects. Dedham, MA: Artech House, Inc, 1975.

13. "Ground-based Space and Missile Warning Sensor Characteristics" (U). Technical Memorandum 84-S-1, HQ SPACECMD, Colorado Springs, CO, July 1984.

14. Hausz, Walter. "Angular Location, Monopulse and Resolution." Radars, Vol 4, Radar Resolution and Multi-path Effects. Dedham, MA: Artech House, Inc, 1975.

15. Herrick, Samuel. Astrodynamics. London: Van Nostrand Reinhold Co.; Vol. 1, 1971; Vol. 2, 1972.

16. Ksienski, Aharon A. and Robert B. McGhee. "A Decision Theoretic Approach to the Angular Resolution and Parameter Estimation Problem for Multiple Targets." Radars, Vol 4, Radar Resolution and Multi-path Effects. Dedham, MA: Artech House, Inc, 1975.

17. "PAM Important in Shuttle Transition." Aviation Week and Space Technology, 113: 82-83 (Nov 17, 1980).

18. Pollon, Gerald E. and Gerald W. Lank. "Angular Tracking of Two Closely Spaced Radar Targets." Radars, Vol 4, Radar Resolution and Multi-path Effects. Dedham, MA: Artech House, Inc, 1975.

19. "Reconnaissance/Surveillance Space Systems-USSR" (U). Defense Intelligence Agency, Wahington, D.C., 25 March 1985.

20. "Shuttle To Make Direct Orbit Insertion Launch." Aviation Week and Space Technolgy, 120: 46 (Apr 2, 1984).

21. "Soviets Confirm Shuttle Vehicle Effort." Aviation Week and Space Technology, 109: 25 (Oct 16, 1978).

22. "Soviet Shuttle, Heavy Booster in Serious Development Trouble." Aviation Week and Space Technolgy, 122: 21-22 (May 27, 1985).

23. "Space Surveillance Network Handbook" (U). Contract F05604-82-C-0075. Science Applications, Inc., Colorado Springs, CO, 7 August 1984.

24. Taff, Laurence G. Celestial Mechanics. New York: John Wiley & Sons, 1985.

VITA

Edward Franklin Faudree, Jr. was born on 15 October 1955 in Jacksonville, Florida. He graduated from high school in Goochland, Virginia in 1974 and attended the University of Virginia from which he received the degree of Bachelor of Arts in physics and astronomy in May 1978. Upon graduation, he received a commission in the USAF through the ROTC program. He was employed as a teacher for the Math and Science Center, Richmond, Virginia until called to active duty in January 1979. He was an orbital analyst at NORAD, Cheyenne Mountain Complex, Colorado until January 1981. He then served as an instructor with Air Training Command at Peterson AFB, Colorado until September 1982 and at Lowry AFB, Colorado until May 1984 when he entered the School of Engineering, Air Force Institute of Technology.

Permanent address: Rt. 1, Box 244
Manakin-Sabot, Virginia 23103

UNCLASSIFIED

SECURITY CLASSIFICATION OF THIS PAGE

REPORT DOCUMENTATION PAGE

1a. REPORT SECURITY CLASSIFICATION: unclassified

1b. RESTRICTIVE MARKINGS: N/A

2a. SECURITY CLASSIFICATION AUTHORITY:

2b. DECLASSIFICATION/DOWNGRADING SCHEDULE:

3. DISTRIBUTION/AVAILABILITY OF REPORT: Approved for public release; distribution unlimited

4. PERFORMING ORGANIZATION REPORT NUMBER(S): AFIT/GSO/ENS/85D-9

5. MONITORING ORGANIZATION REPORT NUMBER(S):

6a. NAME OF PERFORMING ORGANIZATION: School of Engineering, Air Force Institute of Technology

6b. OFFICE SYMBOL (If applicable): AFIT/ENS

7a. NAME OF MONITORING ORGANIZATION:

6c. ADDRESS (City, State and ZIP Code): Wright-Patterson AFB, OH 45433

7b. ADDRESS (City, State and ZIP Code):

8a. NAME OF FUNDING/SPONSORING ORGANIZATION:

8b. OFFICE SYMBOL (If applicable):

9. PROCUREMENT INSTRUMENT IDENTIFICATION NUMBER:

8c. ADDRESS (City, State and ZIP Code):

10. SOURCE OF FUNDING NOS.

PROGRAM ELEMENT NO.	PROJECT NO.	TASK NO.	WORK UNIT NO.

11. TITLE (Include Security Classification): See Box 19

12. PERSONAL AUTHOR(S): Edward F. Faudree, Jr. Captain, USAF

13a. TYPE OF REPORT: MS Thesis

13b. TIME COVERED: FROM ________ TO ________

14. DATE OF REPORT (Yr., Mo., Day): 1985 December

15. PAGE COUNT: 88

16. SUPPLEMENTARY NOTATION:

17. COSATI CODES

FIELD	GROUP	SUB. GR.
22	03	

18. SUBJECT TERMS (Continue on reverse if necessary and identify by block number): Space shuttles; space surveillance systems

19. ABSTRACT (Continue on reverse if necessary and identify by block number)

From Box 11. FEASIBILITY STUDY OF SURVEILLANCE AVOIDANCE DURING THE DEPLOYMENT OF SOVIET PAYLOADS OF MILITARY INTEREST INTO ORBIT FROM A SOVIET SHUTTLE.

Thesis Advisor: Maj. William F. Rowell

20. DISTRIBUTION/AVAILABILITY OF ABSTRACT: UNCLASSIFIED/UNLIMITED ☒ SAME AS RPT. ☐ DTIC USERS ☐

21. ABSTRACT SECURITY CLASSIFICATION: unclassified

22a. NAME OF RESPONSIBLE INDIVIDUAL: William F. Rowell, asst prof ops res

22b. TELEPHONE NUMBER (Include Area Code): (513) 255-3362

22c. OFFICE SYMBOL: AFIT/ENS

DD FORM 1473, 83 APR EDITION OF 1 JAN 73 IS OBSOLETE.

UNCLASSIFIED

SECURITY CLASSIFICATION OF THIS PAGE

Abstract

This ~~work concerns how easily~~ the North American Aerospace Defense Command's (NORAD) radars can detect a satellite deployment from a Soviet space shuttle, one that is comparable to the U.S. space shuttle in size and capability. The radar locations and capabilities were assumed to be the ones presently operating plus a new PAVE PAWS radar in Texas and a new mechanical tracker on the island of Saipan. All radars were assumed to be in working order, and tracking the shuttle.

The shuttle was assumed to be launched in a 51.62° inclination, and would attempt deployment only at an ascending or descending node. The satellite could move away from the shuttle along the shuttle's radius vector, velocity vector, or angular momentum vector, so that it is approx- imately 50 kilometers from the shuttle one half an orbital revolution later. The geocentric angular separation, absolute distance apart and range difference is calculated when the pair are closest to the radar. The elevation angle above the radar's horizon is estimated, and assuming the worst-case viewing geometry of the shuttle and satellite by the radar site, a topocentric range difference and angular separation are determined. These values of angle and distance are compared to that particular radar's capabilities and if the range and angle are much larger, approximately equal to, or less, than the sensor's limiting range and beamwidth, then the probability of detection is labeled high, medium or low, respectively. This determines the best opportunities the USSR has to deploy a satellite undetected by U.S. radars. The first 30 orbital revolutions are so examined. An orbital maneuver burn of a naval surveillance satellite at a selected deployment opportunity is tested, leading to its detection by the next radar that has an opportunity to view the shuttle and satellite.

This leads to the conclusion that the USSR has little chance to deploy a satellite by a space shuttle and have it go undetected, if the NORAD sensors are available for actively searching for this deployment.

END

DTIC

6-86